HHS Public Access

Author manuscript

Cell Metab. Author manuscript; available in PMC 2017 June 14.

Published in final edited form as:

Cell Metab. 2016 June 14; 23(6): 1093–1112. doi:10.1016/j.cmet.2016.05.027.

Effects of Sex, Strain, and Energy Intake on Hallmarks of Aging in Mice

Sarah J. Mitchell[1], **Julio Madrigal Matute**[2], **Morten Scheibye-Knudsen**[1,3,4], **Evandro Fang**[3], **Miguel Aon**[5], **José A. González-Reyes**[6], **Sonia Cortassa**[5], **Susmita Kaushik**[2], **Marta Gonzalez-Freire**[1], **Bindi Patel**[2], **Devin Wahl**[1], **Ahmed Ali**[1], **Miguel Calvo-Rubio**[6], **María I. Burón**[6], **Vincent Guiterrez**[1], **Theresa M. Ward**[1], **Hector H. Palacios**[1], **Huan Cai**[7], **David W. Frederick**[8], **Christopher Hine**[9], **Filomena Broeskamp**[10], **Lukas Habering**[10], **John Dawson**[11,12], **T. Mark Beasley**[11,12], **Junxiang Wan**[13], **Yuji Ikeno**[14], **Gene Hubbard**[14], **Kevin G. Becker**[15], **Yongqing Zhang**[15], **Vilhelm Bohr**[3], **Dan L. Longo**[15], **Placido Navas**[16], **Luigi Ferrucci**[1], **David A. Sinclair**[17], **Pinchas Cohen**[13], **Josephine M. Egan**[7], **James R. Mitchell**[9], **Joseph A. Baur**[8], **David B. Allison**[11,12], **R. Michael Anson**[1], **José M. Villalba**[6], **Frank Madeo**[10], **Ana Maria Cuervo**[2], **Kevin J. Pearson**[1,18], **Donald K. Ingram**[19], **Michel Bernier**[1], and **Rafael de Cabo**[1,*]

[1]Translational Gerontology Branch, Intramural Research Program, National Institute on Aging, NIH, 251 Bayview Blvd., Suite 100, Baltimore, MD 21224, USA

[2]Department of Developmental and Molecular Biology, Institute for Aging Studies, Albert Einstein College of Medicine, Bronx, NY 10461, USA

[3]Laboratory of Molecular Gerontology, Intramural Research Program, National Institute on Aging, NIH, 251 Bayview Blvd., Suite 100, Baltimore, MD 21224, USA

[4]Department of Cellular and Molecular Medicine, Center for Healthy Aging, University of Copenhagen, Copenhagen, Denmark

[5]Laboratory of Cardiovascular Science, Intramural Research Program, National Institute on Aging, NIH, 251 Bayview Blvd., Suite 100, Baltimore, MD 21224, USA

[*]Correspondence: decabora@mail.nih.gov (R.d.C.).

ACCESSION NUMBERS

Raw microarray data sets have been submitted to the NCBI GEO database under accession number GSE81959.

SUPPLEMENTAL INFORMATION

Supplemental information includes Supplemental Experimental Procedures and associated references, 7 figures, and 6 tables and can be found with this article online at:

AUTHOR CONTRIBUTIONS

R.d.C, D.K.I., K.P, M.B., R.M.A., P.N., D.A.S., L.F., D.L.L., and G.K. conceived and designed the study; S.J.M, J.M.M, M.S-K, M.G-F., D.W., A.A., V.G., T.M.W., and H.H.P performed most experiments; E.F. and V.B. conducted the worm studies while F.B., L.H. and F.M. carried out yeast lifespan studies; M.A. and S.C. ran the metabolomics studies; J.A.G-R., M.C-R., M.I.B., and J.M.V. liver Transmission Electron Microscopy; J.M.M., S.K., B.P., and A.M.C., proteostasis network and associated TEM imaging; H.C., J.M.E., pancreatic islets work; D.W.F. and J.A.B., NAD analysis; C.H. and J.R.M., hydrogen sulfide analysis; J.D., T.M.B. and D.B.A., mouse lifespan analysis; J.W. and P.C., IGF1 and IGFBPs' studies; Y.I. and G.H., histopathology; M.B., K.G.B., and Y.Z., microarray analysis; M.B., R.d.C., S.J.M., M.S-K, M.A., S.C., F.M., J.M.V., and A.M.C. wrote the manuscript and most authors contributed to the editing and proof-reading of the final draft.

[6]Department of Cell Biology, Physiology and Immunology, University of Córdoba, Agrifood Campus of International Excellence, ceiA3, Spain

[7]Laboratory of Clinical Investigation, Intramural Research Program, National Institute on Aging, NIH, 251 Bayview Blvd., Suite 100, Baltimore, MD 21224, USA

[8]Department of Physiology, Institute for Diabetes, Obesity, and Metabolism, University of Pennsylvania, Philadelphia, PA 19104, USA

[9]Department of Genetics and Complex Diseases, Harvard University, Boston, Massachusetts 02115, USA

[10]Institute of Molecular Biosciences, NAWI Graz, University of Graz, and BioTechMed Graz, Graz, Austria

[11]Department of Biostatistics, University of Alabama, Birmingham AL 35294, USA

[12]GRECC, Birmingham/Atlanta Veterans Administration Hospital, Birmingham, AL 35294, USA

[13]Leonard Davis School of Gerontology, University of Southern California, Los Angeles, CA 90089, USA

[14]Barshop Institute for Longevity and Aging Studies, University of Texas Health Science Center at San Antonio, San Antonio, TX 78245-3207, USA

[15]Laboratory of Genetics, Intramural Research Program, National Institute on Aging, NIH, 251 Bayview Blvd., Suite 100, Baltimore, MD 21224, USA

[16]Centro Andaluz de Biologia del Desarrollo, and CIBERER, Instituto de Salud Carlos III, Universidad Pablo de Olavide-CSIC, Sevilla, Spain

[17]Department of Genetics, Harvard Medical School, Boston, MA 02115, USA

[18]Graduate Center for Nutritional Sciences, University of Kentucky, C.T. Wethington Bldg, Rm 591, 900 South Limestone, Lexington, KY 40536, USA

[19]Pennington Biomedical Research Center, Baton Rouge, LA 70809, USA

Abstract

Calorie restriction (CR) is the most robust non-genetic intervention to delay aging. However, there are a number of emerging experimental variables that alter CR responses. We investigated the role of sex, strain, and level of CR on health and survival in mice. CR did not always correlated with lifespan extension, though it consistently improved health across strains and sexes. Transcriptional and metabolomics changes driven by CR in liver indicated anaplerotic filling of the Krebs cycle together with fatty acid fueling of mitochondria. CR prevented age-associated decline in the liver proteostasis network while increasing mitochondrial number, preserving mitochondrial ultrastructure and function with age. Abrogation of mitochondrial function negated life-prolonging effects of CR in yeast and worms. Our data illustrate the complexity of CR in the context of aging, with a clear separation of outcomes related to health and survival, highlighting complexities of translation of CR into human interventions.

Graphical Abstract

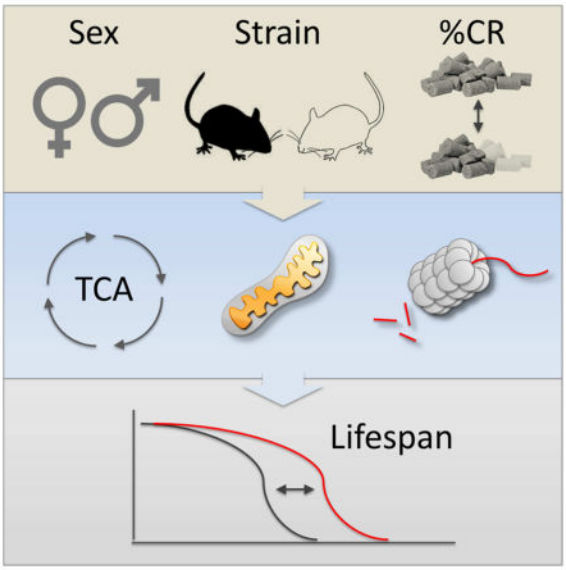

eTOC

In this paper Mitchell et al systematically addresses sex and strain dependent responses to various levels of caloric restriction. Notably, caloric restriction universally increases healthspan through maintenance of energy metabolism and proteostasis with aging. However, there are strain/sex dependent differences in lifespan extension by caloric restriction perhaps uncoupling healthspan and lifespan.

INTRODUCTION

More than a century ago, Moreschi (Moreschi, 1909), Rous (Rous, 1914) observed the beneficial impact of a reduction of caloric intake on transplanted and induced tumors. It was years later when Osborne (Osborne et al., 1917) and then McCay and colleagues reported the lifespan effects of calorie restricted diet in rats (McCay et al., 1935). Since then, calorie restriction (CR) has consistently shown beneficial effects on longevity, age-associated diseases, attenuation of functional decline, and tumorigenesis across a variety of species and diet formulations (Gross and Dreyfuss, 1984; Kritchevsky, 2002; Tannenbaum, 1940; Weindruch and Sohal, 1997; Weindruch et al., 1986). Nevertheless, the exact mechanism(s) underlying these effects remain unknown. Among the most extensively studied hallmarks of CR are enhanced protection against induced and spontaneous carcinogenesis, reduced insulin/insulin-like growth factor 1 (IGF-1) signaling, reduction in oxidative stress and/or increase in antioxidant mechanisms (de Cabo et al., 2004), decrease in different pathologies (Berg and Simms, 1960; Cheney et al., 1980; Ikeno et al., 2013), enhanced mitochondrial function (Lopez-Lluch et al., 2006; Nisoli et al., 2005), improved proteostasis and autophagy (Cuervo, 2008; Hansen et al., 2008), a reduction in body temperature (Rikke et al., 2003) and reduction in reproductive investment (Mitchell et al., 2015b) among others. All these outcomes are accompanied by increases in median and maximum lifespan (Bartke et al., 2007; Gross and Dreyfuss, 1984; Kritchevsky, 2002; Weindruch and Sohal, 1997; Weindruch et al., 1986). These beneficial effects on health and survival have been reported

even after alteration in the macronutrient content and/or restriction of specific components of the diet such as methionine or protein, different feeding regiments and periodic periods of fasting (Fontana and Partridge, 2015; Hine et al., 2015; Masoro, 1990; Miller and Roth, 2007; Murtagh-Mark et al., 1995; Solon-Biet et al., 2015). However, recent evidence suggests that all these tenets may not always hold true. For example, CR does not increase lifespan in all mouse strains (Fernandes et al., 1976; Forster et al., 2003; Goodrick et al., 1990; Harper et al., 2006; Harrison and Archer, 1987; Liao et al., 2010; Liao et al., 2011b; Rikke et al., 2010; Turturro et al., 2002). A remaining question is therefore what factors influence the response to CR.

Traditionally, diet composition and genetic background have been thought to have little influence on the lifespan extension by CR. Recently, data emerging from two independent non-human primate studies challenged this association by reporting similar improvements in health but contrasting survival benefits in response to CR (Colman et al., 2009; Mattison et al., 2012). This uncoupling of lifespan/healthspan benefits by CR has been reported in earlier studies in mice and non-human primates (Colman et al., 2009; Mattison et al., 2012; Rikke and Johnson, 2007; Turturro and Hart, 1991). The notion of a direct correlation between lifespan extension, health and CR, regardless of the context, needs to be revisited. It is becoming clear that, multiple variables should be considered before the optimal implementation of CR. Perhaps, it is possible that the differential responses observed are context dependent, particularly on the interactions between diet, strain, sex and the degree of CR imposed. We posit here that there is an “ideal” context in which CR benefits will be maximized for each individual. Using a comprehensive analysis in this study, we sought to test the impact that genetic background (strain), sex and level of CR have on the traditional response to this intervention and to further elucidate the potential underlying mechanisms linking extension of lifespan and health in mice.

RESULTS

Effects of strain and sex on the healthspan and lifespan of mice on calorie restriction

To determine the role of strain and sex on the lifespan of mice on varying degrees of CR, female and male C57BL/6J and DBA/2J (herein referred to as B6 and D2, respectively) mice were fed Harlan 18% protein diet either *ad libitum* (AL) or at 20 and 40% CR starting at 6 months of age for the remainder of their lives (Figure 1A). In B6 mice, 20% CR significantly improved survival, with a mean lifespan extension of 40.6% in females and 24.4% in males relative to AL-fed controls (Table S1). However, B6 females on 40% CR did not show a beneficial response in survival compared to AL-fed controls (Table S1), and, yet, a modest 13.3% increase in maximum lifespan was observed (Figure 1A), B6 males did show a beneficial effects of 40%CR, but not to the same degree of 20%. D2 mice exhibited 37.3% and 29.8% increases in maximum lifespan in both sexes maintained on 40% CR, respectively (Table S1), even though D2 males on 40% CR had an 18.8% reduction in first quarter (Q1) lifespan, an observation consistent with an earlier report (Forster et al., 2003). Interestingly, D2 females, did not show further benefits from 20% to 40% CR. Thus, the response of these strains to CR shows a clear role of sex, strain and level of CR on survival outcomes.

Mice on CR exhibited reductions in body weight trajectories that were not proportional to the reduction in caloric intake (AL > 20% CR > 40% CR; Figure 1B). Body composition was assessed at baseline (before the onset of CR) and at 12 and 24 months of age (Table S2). D2 males had a considerably higher percentage of body fat than D2 females and B6 mice at baseline, which they maintained throughout their life. By 12 months of age, body fat and lean mass percentages were similar across diet groups; however, strain-specific differences in body composition were apparent at 24 month of age, with CR-fed D2 mice exhibiting the greatest protection against loss in percentage body fat associated with aging (Table S2, Figure 1C). Despite being maintained on 40% CR, 24-months old B6 females had a similar percentage of body fat loss as AL-fed controls. It is possible that the preservation of fat mass in CR mice between 12 and 24 month-old plays a protective role in survival and lifespan extension, in agreement with previous findings (Liao et al., 2011a).

One of the primary physiological responses to CR is the reduction in body temperature (Weindruch et al., 1979) in both rodents (Duffy et al., 1989; Mitchell et al., 2015a; Speakman and Mitchell, 2011), non-human primates (Lane et al., 1995) and humans (Soare et al., 2011). We measured rectal body temperature (T_b) during the dark cycle and found that D2 mice had generally lower T_b compared to B6 mice, with a trend toward T_b reduction with CR versus AL (Figure 1D). A stepwise reduction in T_b with increasing level of CR was observed in male B6 mice, whereas B6 females on 20% CR had a significant elevation in T_b compared to AL and 40% CR (Figure 1D).

Another characteristic feature of CR is the reduction in the type and number of pathologies (Berg and Simms, 1960; Cheney et al., 1980; Ikeno et al., 2013). Any animal that died during the study underwent a necropsy and gross pathological examination to determine the cause of death (Table S3A). A subset of tissues underwent further histopathological analysis by a board certified pathologist blinded to the dietary intervention (Table S3B). In general, there was a delay in the incidence of most commonly occurring pathologies (e.g. lymphoma) in response to CR, as CR-fed animals died at an older age with the same pathologies (Figure 1E, Table S3). Notably, there was a CR dose-dependent decrease in pathologies even in the groups that showed little or no lifespan extension. The incidence of other pathologies such as glomerulonephritis was unchanged across groups (Table S3B), indicating that CR can only delay the onset of age-related diseases but not fully prevent pathologies associated with aging.

CR attenuates age-associated impairments in glucose homeostasis and maintains pancreatic islet morphology

One of the proposed mechanisms of CR-mediated lifespan extension is the maintenance of insulin sensitivity (Barzilai et al., 1998). We measured markers of insulin sensitivity, namely circulating glucose, insulin, leptin, and adiponectin in mice either maintained on AL, 20% or 40% CR (Table S4). Glucose and insulin levels were lower and appeared to plateau in B6 females maintained on 20% CR versus AL. While CR-fed D2 females exhibited a dose-dependent decrease in blood glucose with no changes in circulating insulin, B6 and D2 males on CR showed a stepwise reduction in glucose and insulin levels (Table S4). The Homeostatic measure of insulin resistance (HOMA-IR) was significantly lower with CR

across the experimental groups, plateauing at 20% CR (Figure 1F and Table S4). We measured fasting serum IGF-1 and IGFBP-1 in mice (Table S4) and found a reduction in IGF-1 levels with increasing level of CR regardless of the mouse sex or strain, which is in agreement with previous reports (Anson et al., 2003; Breese et al., 1991; Mitchell et al., 2015b). The long-term effects of CR on circulating IGFBP-1 levels are paradoxical, with increased concentrations in humans (Fontana et al., 2016), but a significant decrease in rodents when compared to AL-fed controls (Breese et al., 1991). Here, serum IGFBP-1 was higher in CR-fed D2 mice and B6 females on 40% CR, but was lower in CR-fed B6 males and B6 females on 20% CR than in their AL-fed controls (Table S4). In contrast, circulating adiponectin was higher and leptin was lower with both degrees of CR than in the AL-fed groups regardless of mouse strain and sex (Table S4). CR was associated with a dose-dependent increase in adiponectin levels relative to AL-fed mice, except for B6 females where adiponectin levels plateaued with 20% CR. Circulating levels of leptin were reduced in B6 mice on CR, consistent with a recent report (Mitchell et al., 2015b). Notably, leptin levels were much lower in the AL-fed D2 females than in all other groups of mice on AL, consistent with the fact that D2 female mice had the lowest percentage of body fat mass (Table S2). Leptin levels are negatively correlated with level of CR in B6 male mice (Mitchell et al., 2015b). This was consistent with our study (data not shown) in both male and female B6 mice, but not D2 mice, highlighting the complexity in the physiological response to CR across different strains of mice.

To further investigate glucose homeostasis we examined pancreatic islet area and found a significant reduction in 17–23 month-old mice on CR compared to AL-fed controls (Figure 1G and 1H). The ratio in the number of alpha/beta cells was significantly lower with CR, indicating that the process of islet hypertrophy that occurs as a consequence of aging (Figueroa and Taberner, 1994) appears to be ameliorated with CR independent of mouse strain and sex.

Transcriptional profiling of the effect of varying degrees of CR on liver gene expression

The liver is essential for the maintenance of metabolic homeostasis and the resulting energetic balance of the organism. Therefore, to further define the pathways and genes that were affected by CR, we performed whole-genome microarray analysis on liver samples of 2-year-old male and female B6 and D2 mice. Principal component analysis (PCA) showed a clear effect of strain (PC1) and CR (versus AL feeding; PC2) on liver transcriptome for both females (Figure 2A) and males (Figure 2B). To understand the determinants responsible for the unique lifespan trajectories in response to CR, four-way Venn diagrams were plotted with the four CR20-AL (Figure 2C and 2D) and CR40-AL (Figure 2F and 2G) pairwise comparisons. The number of transcripts that were upregulated (Figure 2C and 2F) and downregulated (Figure 2D and 2G) are depicted, with more than 262 shared transcripts (139 upregulated and 123 downregulated) in response to 20% CR and 290 shared transcripts (141 upregulated and downregulated) with 40% CR as compared to AL-fed littermates. Parametric analysis of gene set enrichment enabled the identification of significantly altered gene sets in the CR20-AL, CR40-AL and CR40-CR20 pairwise comparisons, and these included the upregulation of pathways implicated in fatty acid metabolism, mitochondrial bioenergetics, and Phase II conjugation and the downregulation of gene sets associated with

genome integrity, transcription, and inflammation (Figure 2E and 2H). Canonical pathways related to fatty acid metabolism and the top twenty CR-regulated transcripts in the four CR40-CR20 pairwise comparisons are depicted in Tables S5A and S5B, respectively. Figure 2I depicts a binary representation of gene expression related to mitochondrial electron transport chain among all 24 pairwise comparisons, where the effect of diet, mouse strain and sex was evaluated. Similar representation of gene expression related to fatty acid metabolism and core components of nucleosome is shown in Figure S1. Another important effect observed in the analysis of these data was the down regulation by CR of major urinary proteins (MUPs), consistent with a reduction in their reproductive capacity (Figure S1C). This family of proteins is directly linked to reproduction and the energetic switch between reproduction and somatic protection (Kirkwood, 2002). The decrease in MUPs observed herein with CR is consistent with recently published data in B6 males (Mitchell et al., 2015b). In our study, these effects were more pronounced in males than females, particularly in B6 mice, suggesting that CR may lead to somatic sparing while sacrificing reproductive fitness.

Metabolomics and the catabolic mode of liver metabolism under CR

The effect of CR on metabolite profiles in the livers of D2 and B6 mice was characterized, with more than 149 metabolites identified. These were grouped by metabolic signatures (e.g., energy components, fatty acids, vitamins, etc.), and their profiles compared between all 12 groups of mice. As an amphibolic organ, the liver can function both catabolically and anabolically. Under these conditions, the anaplerotic filling (replenishing) of the TCA cycle together with the energetic fatty acid fueling of mitochondria suggests less metabolic reliance on glucose (Figure 3A). Consequently, we interrogated the metabolite profiles for predominance of catabolic or anabolic modes during CR regimens. The profile of metabolites feeding the TCA cycle showed accumulation in CR over AL groups depending on strain and sex as could be judged by the analysis of metabolites' ratio (CR20/AL and CR40/AL) (Figure 3B and 3C). Interestingly, two-way ANOVA of metabolite levels enabled us to distinguish between the clear cut effect of CR in D2 vs. B6 strain, as can be judged from the non-significant interaction between CR and sex in D2 mice (Table S6 and Figure S2A). This result suggests a dependence of the effects of CR on the strain genetic background.

There was accumulation of a remarkably wide range of amino acids, ketogenic (e.g., Phe, Tyr, Ileu) and gluconeogenic (e.g., Gly, Thr, Asp, Met) including branched-chain (BCAAs, Val, Ileu, Leu) and essential (e.g., Val, Ileu, Leu, Lys, Met, Phe, Thr) amino acids (Figure S2B). The levels of most common circulating fatty acids were significantly enhanced as well, such as palmitic, oleic, myristic, stearic and linoleic, along with glycerol, which represents the backbone of triacylglycerols. Other metabolites substantially elevated were glutamate, glutamine, 3-hydroxybutyrate (a ketone body) as well as intermediaries of the TCA cycle such as citrate, malate and fumarate. Ornithine and fumarate accretion are in agreement with activation of the urea cycle to also feed the TCA cycle with fumarate (Figure S2B). In summary, these data support the notion that CR leads to mobilization of peripheral energy deposits that the liver can subsequently utilize for gluconeogenesis.

Hydrogen sulfide and the control of protein handling systems

Hydrogen sulfide (H_2S) production via the transsulfuration pathway is an evolutionarily conserved response to CR that may mediate multiple CR-like benefits, including stress resistance and longevity (Hine et al., 2015). We found a dose-dependent hepatic production of H_2S across B6 and D2 mice in response to CR (Figure 4A and 4B). A heat map generated from metabolomics analysis of liver samples was used to communicate relationships between the 12 experimental groups and 6 major metabolites implicated in the transsulfuration pathway. Clear strain- and sex-specific differences in the patterns of changes in metabolite levels were observed (Figure S3A). The ability of CR to promote elevated levels of hepatic H_2S production was consistent with previous findings (Hine et al., 2015) and may represent a global effect of CR in inducing stress resistance.

The beneficial effects of H_2S on cellular aging may be mediated through the transcription factor Nrf2 and Cyp2a5 detoxification (Abu-Bakar et al., 2007; Chattopadhyay et al., 2012; Yang et al., 2013). Indeed, CR significantly increased *Cyp2a5* mRNA levels independently of mouse strain and sex (Figure 4C), consistent with the H_2S results.

Like CR, H_2S increases lifespan in *C. elegans* (Miller and Roth, 2007) and promotes redox regulation of SIRT1 (Zee et al., 2010) to help maintain the circadian rhythm of mouse hepatocytes (Shang et al., 2012). In our study, SIRT1 protein levels were found to be reduced with 20% CR in B6 females, but remained largely unaffected in other groups except for the significant increase in D2 males on 40% CR (full immunoblot images depicted in Figure S3B, quantitative analysis in Figure 4D, n=6). Poly(ADP-ribose) polymerase 1 (PARP-1), a nuclear DNA repair enzyme that consumes NAD^+, was significantly reduced with CR (exception of D2 females on 40% CR) (Figure 4D, Figure S3B). Although PARP-1 activity was not measured, it is possible that CR-induced changes in PARP-1 expression will impact on the NAD^+ levels, thereby affecting protein deacetylation performed by sirtuins and ultimately shape nuclear-mitochondrial communication and the control of energy homeostasis (Canto et al., 2015; Gomes et al., 2013; Guan and Xiong, 2011). We observed that CR hindered to a certain extent the age-related reduction in hepatic NAD^+ level, although it did not reach statistical significance (Figure 4E). Consistent with the report of Schwer et al. (Schwer et al., 2009), the global pattern of lysine acetylation and deacetylation in liver lysates was refractory to CR-mediated protein deacetylation (Figure 4D, Figure S3B), as evidenced by the fact that the ratio of acetylated to total p53 was significantly increased with CR (Figure 4D, Figure S3B). The acetylation ratio of SOD2 differed in relation to sex and strain, with 20% and 40% increases in B6 males and D2 females, respectively, which is similar to their lifespan increases with CR. The increase in SOD2 acetylation level at steady-state occurred despite higher expression of the deacetylase SIRT3 in CR samples (Figure 4F, Figure S3C). These results are consistent with CR-mediated inhibition of SIRT3 and are at odds with previous reports (Qiu et al., 2010; Tauriainen et al., 2011). Alternatively, acetylation changes could be caused by increase in acetyl-CoA levels in the liver, a phenomenon that is known to occur with fasting.

NAD(P)H:quinone oxidoreductase 1 (NQO1), a key player in the antioxidant and detoxification pathways, is a Nrf2 target protein inducible by H_2S (Chattopadhyay et al., 2012). We found that CR treatment caused a dose-dependent increase in NQO1 protein

levels irrespective of sex and strain; however, the magnitude of this increase was much lower in D2 males on 40% CR (Figure 4G, Figure S3D). NQO1 also functions as a gatekeeper protein capable of competing with the 20S proteasome for interaction with different proteins (Moscovitz et al., 2015). Binding of NQO1 to the key metabolic regulator PGC-1α leads to its stabilization and protection against proteasomal degradation (Adamovich et al., 2013). Here, we found a trend towards higher PGC-1α levels in response to CR, consistent with PGC-1α stabilization –as a consequence of NQO1 induction- and subsequent increase in the levels of mitochondrial transcription factor A (TFAM) (Figure 4G, Figure S3D). Of significance, the size and density of mitochondria were found to be significantly higher in response to CR (see below, Figure S6B). Albeit refractory to CR, the acetyl-CoA carboxylase (ACC) levels showed a clear dependence on sex and strain whereas AMPK levels trended toward higher expression with CR (Figure 4G, Figure S3D), in support of an AMPK-mediated increase in mitochondrial fatty acid oxidation. FOXO3a is a downstream target of AMPK that has a role in stress resistance, glucose metabolism, and apoptosis; FOXO3 levels mirrored those of AMPK protein (Figure 4G, Figure S3D). The deficiency in thioredoxin-interacting protein (TXNIP) causes the disruption of the fasting-feeding metabolic transition (Sheth et al., 2005) and whole body energy metabolism (DeBalsi et al., 2014). Here, TXNIP protein expression pattern increased with the degree of CR in all groups except for D2 males on 20% CR (Figure 4H, Figure S3D). Taken together, these data illustrate the contribution of sex and strain to the altered metabolism and promotion of stress resistance by CR, which, in turn, confer health and lifespan benefits.

CR and the regulation of the ubiquitin-proteasome pathway and autophagy

The effects of sex and strain on CR-induced changes in major protein degradation systems, which include the ubiquitin-proteasome pathway and autophagy, were explored. Attachment of ubiquitin molecules to proteins is commonly used for their degradation by the 26S proteasome complex (when using the ubiquitin K48-linkage) or by autophagy (if ubiquitin chains are attached through K63-linkage) (Ciechanover, 2005; Olzmann and Chin, 2008; Tan et al., 2008). We measured the degree and type of protein ubiquitination in liver homogenates by immunoblot analysis and found that CR induced clear reduction in K48- and K63-linked ubiquitination of soluble proteins especially in males (Figure 5A and 5B). Changes in levels of soluble ubiquitinated proteins upon CR were minimal for the two female groups, and DBA females displayed considerably higher levels of both soluble ubiquitinated proteins and also constitutive accumulation of higher molecular weight polyubiquitinated protein aggregates (depicted as ‘Agg’ in Figure 5A and 5B). Although the observed changes could be a result of differences in the rate of ubiquitination, since cells can cope with proteotoxicity of misfolded proteins by increasing their aggregation or their degradation, we hypothesized that the reduction in ubiquitinated proteins observed in the male groups upon CR could reflect enhanced degradation through the proteasome, whereas D2 females utilize mostly aggregation. We next analyzed both the chymotrypsin-like (CTL) and peptidyl-glutamyl peptide-hydrolytic (PGPH or caspase-like) proteolytic activities of the proteasome in liver homogenates *in vitro* and differentiated between 26S and 20S by supplementing or not the reaction with ATP. Contrary to our prediction of CR-enhanced proteasome degradation in males, these studies revealed significant reduction of proteasome activity in all groups in response to CR (Figure 5C and 5D). This CR-induced inhibition of

the proteasome activities was overall more pronounced in D2 females, especially in agreement with their higher content of both soluble and aggregate ubiquitinated proteins. When proteasomal activity was measured in the absence of ATP, most of the CR-induced alterations in chymotrypsin-like and caspase-like values were eliminated suggesting less effect of CR on 20S proteasome activities (Figure S4A and S4B). Control experiment illustrated that preincubation of the liver homogenates with the potent proteasome inhibitor MG115 markedly suppressed protease activities measured in the absence or presence of ATP (Figure S4C).

Since the CR-induced reduction in polyubiquitinated proteins could not be attributed to enhanced proteasome activity, we next explored possible changes in autophagic pathways. CR has been shown to prevent the age-dependent decline in macroautophagy activity in rodent liver (Bergamini et al., 2003) and to upregulate autophagy-related genes and proteins in human skeletal muscle (Yang et al., 2016). Ubiquitinated proteins are amenable to degradation via macroautophagy and blockage of this pathway leads to intracellular accumulation of K48 and K63 positive aggregates (Hara et al., 2006; Olzmann and Chin, 2008; Tan et al., 2008). Analysis of steady-state levels of LC3-II, the most commonly used marker to measure autophagic compartments (Kabeya et al., 2000), revealed that 40% CR significantly increased levels of LC3-II in B6 mice when compared to 20% CR (Figure 5E and 5F). A trend toward increased levels of LC3-II in D2 mice on CR was also noticeable although it did not reach statistical significance. Increased levels of LC3-II could be indicative of increased autophagy induction or reduced autophagic flux (autophagosome/lysosome fusion). We next attempted to measure *ex vivo* rates of autophagic flux by changes in levels of LC3-II upon incubation of liver explants with protease inhibitors (Figure 5E and 5G). CR did not modify rates of LC3-II turnover, except for D2 females on 20% CR which displayed significant reduction in LC3-II flux (Figure 5E and 5G). These findings suggest that the CR-induced increase in LC3-II levels was not a consequence of blockage of autophagosome clearance but rather was due to autophagy induction. To further test this possibility, we analyzed the autophagic compartments in transmission electron microscopy (TEM) images of livers from mice on varying degrees of CR (Figure S4D-M). In agreement with the steady-state levels of LC3-II (Figure 5F), morphometric analysis revealed an expansion in number and size of autophagic vacuoles in animals subjected to CR. This increase was, however, more noticeable in the B6 females and D2 males (Figure S4D–G and I–L). Scoring of autophagic vacuoles as autophagosomes or autolysosomes (mature autophagosomes), using standard morphological criteria, revealed that the CR-induced expansion of the autophagic compartments in B6 females and D2 males was a result of increased numbers of both autophagosomes and lysosomes, in further support that CR induced autophagy in these groups (Figure S4F and S4K). Interestingly, all CR livers displayed a significant increase in lipid droplets with morphological signatures of lipophagy (Singh et al., 2009), which was rarely observed in the AL groups (Figure S4H and S4M). D2 males on CR had the highest frequency of lipophagy despite autophagic rates being comparable to those in CR-fed B6 females, which suggests possible differences in the type of autophagic cargo favored by each group.

To complete our analysis of the autophagic system, we also analyzed the effect of CR on hepatic chaperone-mediated autophagy, which has been shown to contribute to metabolic

regulation *in vivo* (Schneider et al., 2014) and restore chaperone-mediated autophagy reverse aging phenotypes in liver (Zhang and Cuervo, 2008). The subpopulation of lysosomes normally active for CMA (those that contain the hsc70 chaperone in their lumen (Cuervo et al., 1997) was isolated from the livers of each of the groups and their chaperone-mediated autophagy activity was compared using a well-established *in vitro* system. We did not find differences among the different groups in the ability of chaperone-mediated autophagy active lysosomes to take up and degrade a pool of radiolabeled chaperone-mediated autophagy substrates (Figure 5H). In agreement with these findings, the levels of the two limiting chaperone-mediated autophagy lysosomal components, LAMP-2A (the CMA receptor) and lysosomal hsc70, remained unchanged upon CR in CMA-active lysosomes (Figure 5I, J and Figure S5). Interestingly, analysis of the same proteins in lysosomes with usual low CMA activity (CMA-) revealed that CR significantly increased levels of hsc70 in this group of lysosomes in the B6 males (Figure 5I) but not in the other groups of mice (Figure 5J and Figure S5). We confirmed using the *in vitro* assay that the higher abundance of hsc70 in the CMA-lysosomes from B6 males, when subjected to CR, increased their ability to perform CMA (Figure 5K shows proteolysis in intact lysosomes that recapitulates binding/uptake and degradation of proteins). Overall, these studies illustrate strain and sex differences in the effect of CR on the different proteolytic systems in liver. Upregulation of different autophagy pathways by CR may contribute not only to the maintenance of protein homeostasis but also to improvements in hepatic carbohydrate and lipid metabolism directly through lipophagy (Singh et al., 2009) or through selective degradation of metabolic enzymes via chaperone-mediated autophagy (Schneider et al., 2014), which have a positive impact on the overall energetic balance of the organism.

Functional mitochondria are required for the life extension benefits of CR

The signature of transcripts that encode key enzymes implicated in energy metabolism pathway was found to be rather complex in response to CR, with *Fh1* (mitochondrial fumarate hydratase) levels significantly increased in B6 and D2 females, but not males; whereas expression of *Pkm* (pyruvate kinase muscle isozyme) transcript was reduced only in CR-fed B6 male and female mice (data not shown). Quantitative RT-PCR analysis showed the significant increase in *Fh1* mRNA levels in B6 and D2 females on CR (Figure 6A) and selective reduction in *Mdh2* (mitochondrial malate dehydrogenase 2) expression in B6 females on 40% CR (Figure 6B). Mdh2 affects the malate-aspartate shuttle and increases cellular anti-oxidant function. However, Western blot analyses and *in vitro* enzymatic activity performed with liver lysates demonstrated that the total amount of MDH2 and its associated activity were significantly increased in all CR-fed groups of mice (Figure 6C and 6D), perhaps suggesting up-regulation of TCA cycle activity consistent with the metabolomics data.

The role of select enzymes implicated in mitochondrial respiration was then examined for their life-enhancing benefits in lower organisms. Based on our array and validation data, we selected *Fh1* and *Mdh2* because were differentially altered in B6 females. When maintained in the absence of food or fed with standard laboratory diet (Figure S6A), *fem-1 (hc17)* and Cy303 strains of *C. elegans* harboring genetic deletion (RNAi feeding) in either *fum*-1 (worm homolog of *Fh1*), *glna*-2 (worm homolog of glutaminase 2) or *mdh2* lived

significantly shorter than wild-type individuals, as evidenced by their reduced mean and median lifespan (Figure 6E–6G). Moreover, the absence of a mitochondrial genome in rho0 yeast cells severely reduced lifespan when fed either AL or CR diet, and was accompanied by significantly higher proportion of PI-positive yeast cells among rho0 cells compared to wild-type cells (Figure 6H). We further tested whether survival required *FUM1 and MDH2*, the yeast homolog of *Fh1* and *Mdh2*. Deletion of FUM1 rendered the cells unresponsive to the prolongevity effects of CR observed in wild-type yeast cells (Figure 6I). The impact of Δ*mdh2* was generally milder with some lifespan extension in response to CR (Figure 6J). These results confirmed the essential requirement of functional mitochondria in the life-extending properties of CR. To further elucidate the potential role of the mitochondria in the unexpected response of B6 female mice to 40% CR, we produced cohorts of B6D2F1 and D2B6F1 offspring and placed them on 40% CR. Currently, with 25% of the cohorts dead, and based on an interim analysis of survival, there is a significant difference between the two F1 hybrid strains, whereby mice that inherited the B6 mitochondrial pool have a clearly diminished response to 40% CR (Figure 6K). Thus, the mitochondria function and haplotype play an essential role in the ability of model organisms to maximally reap the survival effects of CR.

To further assess the impact of CR on mitochondria, transmission electron microscopy (TEM) of livers was carried out, and representative images are shown in Figure 6L. From these images, we obtained both planimetry and stereological data to characterize morphology of liver mitochondria in the experimental groups. There were significant changes in mitochondrial size depending on sex and strain. Remarkably, an increase of mitochondrial size was found in B6 and D2 males and in B6 females fed a 40% CR diet, but no increase was observed in D2 females fed the same diet (Figure S6B). With respect to 20% CR, mitochondrial size showed no or only a minor change in males from both strains, while unique patterns were observed in females, with a decrease in B6 and an increase in D2 mice. In contrast, the effect of CR on mitochondrial circularity was consistent in all experimental groups, with a marked decrease of circularity in 20% CR, and a further decrease by 40% CR (Figure S6B), suggesting either increased mitochondrial biogenesis or possibly increased mitochondrial fusion. Stereological analysis was performed to obtain cell volume density (Vv), representing the cell volume fraction occupied by mitochondria per hepatocyte volume unit. For this parameter, the most consistent change was the increase by 40% CR in all groups regardless of strain or sex. In the case of 20% CR, we also observed a general trend towards an increase of Vv, although statistically significant differences were only found for B6 males and D2 females (Figure S6B). Since the increase of nuclear size is a well-established marker of aging in liver (Gregg et al., 2012), we also measured this parameter to assess if the observed structural changes in mitochondria were related with the improvement of liver preservation. Of note, the effects of dietary interventions on hepatocyte nuclear size paralleled those on mitochondrial circularity and roughly mirrored the changes in Vv, since a decrease of nuclear size was observed to occur in all groups, both with 20% and 40% CR, this latter intervention producing a more pronounced effect (Figure S6B).

No discernible differences in citrate synthase activity were observed except for a reduction in female B6 and D2 mice on 40% CR compared to AL controls (Figure S6C). Blue native electrophoresis was used to separate intact mitochondrial electron transport chain complexes

in liver extracts, and the results indicated a significant increase in the levels of respiratory chain complexes I, II and III in CR-fed D2 females, whereas males and females B6 on 40% CR showed higher complex I and II levels, respectively (Figure S6D and S6E). Optimal activity of complex I requires the interaction with prohibitin (Phb), a major mitochondrial inner membrane protein implicated in cristae morphogenesis and functional integrity of mitochondria (Artal-Sanz and Tavernarakis, 2009; Merkwirth et al., 2008). A significant reduction in Phb levels was observed in B6 and D2 males in response to CR, which was in sharp contrast to the 3–4.5-fold increase in the amount of Phb protein in CR-fed D2 females (Figure S6F and S6G). This event did not occur in B6 females on CR. Strikingly, the expression of the classical mitochondrial cochaperone Hsp60 was severely abrogated in B6 and D2 females, but not males (Figure S6F and S6G). These results indicate sex-specific differences in the metabolic regulation of mitochondrial architecture and function, which likely results in distinct variation in healthy aging and lifespan extension.

Global hierarchical clustering

To further analyze the extensive amount of data presented here and to obtain a global unbiased understanding of which factors might contribute to longevity, we performed principal component analysis (PCA) of Z-score-normalized behavioral, physiological and biochemical data (Figure 7A and S7). Notably, the strongest principal component (PC1) appeared to be the dietary intervention while PC2 appeared to describe changes associated with strains supporting the notion of a universal response to dietary interventions across B6 and D2 mice. We further performed hierarchical clustering (Figure 7B) of this data that revealed good separation between AL-fed groups and the CR groups and, interestingly, seemed to facilitate association between the groups that had the greatest benefit of lifespan (CR20B6F, CR20B6M and CR40B6M) and those that had less benefit (CR40B6F, CR20D2F, CR40D2F, CR20D2M, CR40D2M) (Figure 7B). Notably, by performing the same analysis on the input data, the closest association to maximum lifespan was fat mass while NAD+ levels appeared to correlate the strongest with mean lifespan (Figure S7). These data support the findings that maintenance of mitochondrial function, NAD^+ levels and preservation of essential fat mass with age are important predictors of lifespan.

DISCUSSION

Calorie restriction has long been the measuring stick and gold standard for alternative strategies to improve health and survival in biomedicine by manipulating cellular and molecular mechanisms of aging. However, emerging evidence calls into question the universality of the effects of CR in extending mean and maximal lifespan. These life extension effects may be influenced by common experimental variables such as species, genetic background, sex, macro-nutrient composition and meal timing, degree of restriction, age of onset and their interactions. In this study, we have systematically addressed the effects on health and survival of three factors: genetic background, sex, and degree of CR, and examined key physiological hallmarks of the CR response (body weight, core body temperature, insulin sensitivity, metabolism, pathology and survival) to determine if there is an optimal level of CR that will maximize health and survival in two strains of mice for both sexes. Our results provide further evidence that multiple factors alter the response to CR and

that while the effect of CR on health appeared consistent across strains and sexes, but survival was not correlated with CR in all cases.

The universal effects of CR on lifespan were challenged recently in a number of studies in wild-derived mice (Harper et al., 2006), inbred strains (Fernandes et al., 1976; Forster et al., 2003; Goodrick et al., 1990; Harrison and Archer, 1987; Turturro et al., 2002) and recombinant inbred strains (Liao et al., 2010; Rikke et al., 2010). Indeed, bodyweight loss and reduction in core body temperature were not proportional to the number of calories consumed or to survival. Mice on CR weighed less than AL-fed controls, although this is not always proportional to their level of restriction. Mice that responded the best on survival outcomes were those that preserved their fat mass better into the second year of life, suggesting that there is a minimum level of adiposity that is necessary for the full benefit of CR and that the contribution of this organ to metabolic regulation under CR condition is crucial. These results are congruent with the work of Liao et al. (2011) showing that strains of mice with lowest reduction in fat under CR were more likely to have extended lifespan. Furthermore, long-lived strains, such as the Ames and Snell dwarf mice, have higher percentages of body fat even though they are smaller than their littermates. Indeed, recent work has shown in humans that slight overweight is associated with the lowest level of all-cause mortality (Flegal et al., 2013; Grabowski and Ellis, 2001)

The recognition that fat tissue is an endocrine organ capable of producing adipokines led us to measure the circulating levels of leptin and adiponectin, two regulators of long-term energy balance (Mitchell et al., 2015b). Serum leptin was lower, but adiponectin was higher in CR-fed mice than in their AL-fed controls, which can be attributed to the reduction in body weight and potential reprogramming of hepatic fat metabolism in response to CR (Kuhla et al., 2013). CR in rodents is also known to reduce fertility, perhaps as an evolutionary response to hunger, enabling the shutdown of reproduction and the investment of all energy into repair mechanisms and survival (Kirkwood, 2002; Kirkwood and Shanley, 2005). Here, we showed a dramatic reduction in expression of liver MUPs, which are linked to maintenance of organ size and male sexual signaling. These changes in MUPs were mostly closely linked to organ size and leptin levels. In accordance, hepatocyte nuclear size, which is known to increase with aging possibly due to enhanced polyploidy (Gregg et al., 2012), was significantly lower in all CR groups compared with their AL counterparts, regardless of sex and strain, indicating a better preservation of liver homeostasis by CR.

The reduction in body temperature (T_b) has been postulated to play a role in the CR-promoting effects on lifespan in rodents and non-human primates (Duffy et al., 1989; Lane et al., 1995; Mitchell et al., 2015a; Speakman and Mitchell, 2011; Turturro and Hart, 1991). Interestingly, strains of mice that maintain high T_b are more likely to have extended lifespan under CR (Speakman and Mitchell, 2011). While this is contradictory to the suggestion that lowered T_b is a contributing factor to lifespan extension under CR (Speakman and Mitchell, 2011), it certainly highlights that there is more complexity to the CR phenomenon, especially when performing comparisons across mouse strain and sex. Our findings are in concordance with previous studies with the exception of B6 female mice on CR. In these mice, T_b was significantly higher with 20% CR than in B6 females on AL or 40% CR. Alteration in heat production or heat loss and change in metabolic rate and/or activity could

account for the increased T_b in B6 female mice on 20% CR. The preservation of fat mass means more insulation and lower rate of health decline as these mice age, which may have contributed in having opposing effects on the classical T_b response to CR (Rikke and Johnson, 2007). Even though metabolic rate or activity level were not measured, it is believed that lower T_b contributes to longevity through direct effect on reducing pathologies (Speakman and Mitchell, 2011). As demonstrated in all experimental groups, with the exception of D2 males, CR feeding induced a reduction in both the number and age of onset of pathologies.

Improvement in insulin sensitivity and signaling via the insulin/IGF-1 signaling pathway is a proposed mechanism through which CR retards aging and promotes lifespan (Milman et al., 2014). Genetic mutations in growth hormone, IGF-1 receptor, or downstream effectors of insulin/IGF-1 signaling (i.e. PI-3 kinase and FOXO) have been associated with increased lifespan (Flurkey et al., 2002; Flurkey et al., 2001; Hsieh et al., 2002; Shimokawa et al., 2015; Sun et al., 2013), data from a study using recombinant inbred strains showed that plasma IGF1 levels were inversely correlated with median lifespan (Yuan et al., 2009b), further we have recently show that high IGF-1 is correlated with increased risk of cancer, and men with low IGF-1 because of GHR deficiency are fully protected against cancer (Guevara-Aguirre et al., 2011). Here, fasting levels of insulin, glucose, and IGF-1 were reduced with CR across all experimental groups, thus representing a global and consistent effect of CR on improving insulin sensitivity (Mitchell et al., 2015b). In most cases 20% CR was sufficient to produce a dramatic decrease in these parameters with little to no further benefit by 40% CR. The reduction in age-associated pancreatic islet hypertrophy combined with enhanced insulin sensitivity and lower insulin levels are likely to represent an important mechanism —although almost certainly not exclusive— by which CR increases longevity (Masternak et al., 2009). Although the levels of IGFBP-1 did not correspond to extended longevity in CR-fed mice, the possibility exists that higher IGFBP-1 helps improve health, while lower IGFBP-1 levels are associated with increased lifespan in response to CR. In this study, the shortest lived animals (B6 females on 40% CR and all CR-fed D2 mice) had very low circulating levels of IGF-1 combined with high circulating IGFBP-1 levels. Indeed, low levels of IGF-1 and muscle mass have been shown to be negatively correlated with decreases in median and maximal lifespan in mice (Sharples et al., 2015; Yuan et al., 2009a).

The integration of physiological outcomes and hepatic transcriptomic and metabolomics data have provided the necessary tools to further examine the contribution of mouse strain and sex and the level of CR toward the lifespan trajectories. The overall buildup of metabolites indicates that the liver of CR-treated mice functions mainly in catabolic mode within mitochondria, with fatty acid β-oxidation catabolically driving the TCA cycle. In addition, a profile consistent with anaplerotic replenishment via amino acids (both ketogenic and gluconeogenic) and the urea cycle via fumarate could be observed. Under these conditions, the anaplerotic filling of the TCA cycle together with the energetic fatty acid fueling of mitochondria render a metabolism relying less on glucose. The apparent depression of intermediate levels of glycolytic, pentose phosphate and glycogen pathways, and the increased insulin sensitivity (e.g., significantly lower HOMA-IR index) exhibited by the CR-treated mice support this notion. In response to CR, liver metabolite profiles showed an enhancement in mitochondrial respiration driven by fatty acid degradation, which was

accompanied by increased expression of respiratory complexes, and which is expected from greater use of fat as fuel source (Bruss et al., 2010), and concomitant alteration in body fat composition.

Consistent with the current literature, our transcriptomic analysis indicated a strong impact of CR on pathways implicated in proteostasis, energy metabolism and mitochondrial bioenergetics. Loss of proteostasis is a common hallmark of aging that has been shown to be prevented by CR (Kaushik and Cuervo, 2015). Although with some sex differences, we found reduced levels of polyubiquitinated proteins with CR that cannot be attributed to enhanced proteasome activity, since the activities of this major cellular protease were instead lower in CR mice. It is possible that reduced overall protein synthesis/ubiquitination contributes to their lower abundance in CR, but we propose that, at least in some species and sex, increased autophagy could be behind the CR-induced proteostasis changes. Beyond its role in protein homeostasis, autophagy has been proven essential for specific adaptation to nutritional availability, both during nutrient excess and scarcity (Madrigal-Matute and Cuervo, 2016). Interestingly, TXNIP has also a role in stress-induced macroautophagy (Qiao et al., 2015), one of the hallmarks of aging. Although CR increased overall autophagic activity in most of the experimental groups, we found marked sex and strain differences in the intensity of this autophagic response and the type of autophagy preferentially induced. Both macroautophagy and chaperone-mediated autophagy contribute to regulate hepatic metabolism but through different mechanisms (Madrigal-Matute and Cuervo, 2016). Macroautophagy directly mobilizes energy stores, such as lipid droplets, and also regulates metabolic flux by controlling mitochondria abundance through mitophagy. Whereas all CR groups showed reduced mitochondria circularity, suggestive of reduced mitophagy, only some of them displayed enhanced lipophagy (Gomes et al., 2011; Twig et al., 2008). It is possible that changes in lipid metabolism are a consequence of the observed increase in chaperone-mediated autophagy activity, which was recently shown to contribute to regulation of hepatic lipid metabolism through the degradation of key enzymes in these pathways (Kaushik and Cuervo, 2015; Schneider et al., 2014). Taken together, our results indicate that the increased bioavailability of amino acids and fatty acids in the liver of CR-fed mice may be derived from activation of autophagic pathways. This metabolic switch could account for the increase in healthspan and lifespan observed in most CR-fed animals.

In mouse hepatocytes we have shown that aging induces a decrease in mitochondrial mass together with reduction in individual mitochondria size and changes in the expression pattern of proteins related to fusion/fission dynamics (Khraiwesh et al., 2014; Khraiwesh et al., 2013; Lopez-Lluch et al., 2006). However, 40% CR alleviated most of these effects by inducing increases in individual mitochondria size and volume fraction occupied by mitochondria. The conclusion was reached that CR results in higher number of more efficient mitochondria. The results reported here show a general increase in mitochondrial mass (expressed as volume density) with CR regardless of sex or strain of mice, although 40% CR appears to have a more pronounced effect on this parameter. In addition, mean mitochondrial size varied depending on the strain, sex and the degree of CR but, with the exception of D2 females, 40% CR induced an increase in mitochondrial area, which fit well with the results reported by Khraiwesh el al (2014) in B6 mice. Moreover, CR was found to uniformly decrease circularity in mitochondria in all of the dietary groups. It has been shown

that mitochondrial shape is closely related to mitophagy in such a way that elongated mitochondria are preserved from mitophagy (Gomes et al., 2011). Therefore, the possibility exists that selective mitophagy (depending on the mitochondrial haplotype) accounts for the preservation of efficient mitochondria in CR-fed animals.

In *C. elegans*, it has been clearly demonstrated that aging induces a decline in mitochondrial function that leads to the activation of specific pathways (Chang et al., 2015) and an increase in reactive oxygen species (ROS). Orthologues of p53 and NRF2 (CEP-1 and Skin1) are among other important mediators of longevity induced by mild mitochondrial dysfunction in the worm. SKN-1 directly associates with the mitochondria and has been shown to be critical to the response to CR. Moreover, we have shown that Nrf2 is essential for the anti-carcinogenic effects of CR in mice (Pearson et al., 2008b). Based on our transcriptomic analysis, we genetically manipulated a selection of these transcripts in yeast and worms to demonstrate that the maintenance of healthy and functional mitochondrial population is necessary for the pro-survival effects of CR in these two organisms. Furthermore, two F1 hybrid strains produced from the cross of B6 and D2 mice responded to 40% CR in a maternally inherited manner, suggesting the importance of the inherited mitochondria pool for the responsiveness to this dietary intervention.

Even if long-term CR was shown to benefit human aging, confer cancer protection, and increase longevity, it would be extremely difficult to achieve adherence to such a stringent diet that might require a reduction of 20–40% in daily caloric intake. Human CR studies have shown clear effects on metabolic and molecular health in humans, reduced multiple risk factors implicated in the pathogenesis of type 2 diabetes, obesity, cardiovascular disease, cancer, stroke, vascular dementia, liver and kidney diseases(Fontana et al., 2014; Longo et al., 2015). More research is needed to fine tune our understating of the pathways implicated and how to precisely modulate them, but the evidence of the protective effects of CR in humans are clear and powerful. To this end, considerable investment has been focused on dissecting the pathways that regulate the beneficial effects of CR to spur development of pharmacological agents potentially acting as CR mimetics. In recent years, dietary regimens, CR mimetics and small molecules have generated promising results in anti-aging trials. Not surprisingly, most of these interventions have strain-, diet-, and sex-specific effects on health and survival in mice (Anisimov et al., 2008; Harrison et al., 2014; Harrison et al., 2009; Martin-Montalvo et al., 2013; Miller et al., 2011; Miller et al., 2014; Pearson et al., 2008a; Strong et al., 2013; Strong et al., 2008). Nonetheless, these molecules are bolstering our understanding about their molecular mechanisms and their use for aging and age-related chronic diseases such as cancer, cardiovascular disease and neurodegenerative disorders. A logical extension of these interventions is aimed at understanding the proper context in which the application of these interventions will be most beneficial to humans, and to identify which biomarkers are associated with the best predictors of healthspan and lifespan. These biomarkers could be part of standard screening protocol to identify earlier and more effective interventions and treatments in the clinic than the current standard of 3+ years in a mouse longevity study. It is through the innovative and unique interdisciplinary approach of geroscience that we will gain further understanding of the biological mechanisms underlying aging and age-related disease and disability. While great strides have been made by scientists engaged in aging research, the recent formation of the Trans-NIH GeroScience

Interest Group, the Intervention Testing Program and other similar groups have served as catalysts for major leaps in this field.

CONCLUSION

CR effects on survival are not universal. We have demonstrated a strain-, sex-, and dose-dependent effect of CR on the health and survival in two strains of mice. It appears that the interaction and contribution of each of these factors may have an impact on the overall energetic balance of the organism, which determines the outcome on health and survival. Our results provide evidence for the complex relationship between health and survival in mouse longevity studies and suggest that to attain the maximal benefits of CR, the maintenance of healthy and functional mitochondria and active autophagy that leads to improvements in carbohydrate and lipid metabolism is required to allow metabolic flexibility and preservation of a healthy amount of body fat into old age.

EXPERIMENTAL PROCEDURES

Animals and diets

Male and female C57BL/6J and DBA2/J mice were obtained from the Jackson Laboratory (Bar Harbor, ME) and then bred in house at the National Institute on Aging (Baltimore, MD) in order to obtain sufficient number of mice per group. In an on-going study, F1 off-springs were bred in house at NIA to generate male B6D2F1/J and D2B6F1/J mice. Litters were maintained with approximately eight pups to minimize the potential confounding effect of a crowded litter (Sadagurski et al., 2014). Mice were housed in cages of three to four with *ad libitum* access to water at the Gerontology Research Center in Baltimore, MD. Mice were fed house chow (2018 Teklad Global 18% Protein Rodent Diet, Harlan Teklad, Indianapolis, IN) either *ad libitum* (AL) or at 20% or 40% CR starting at 6 months of age for the remainder of their lives. F1 offsprings were fed AL and 40% CR and none of the parents used to generate these specific F1 mice underwent CR. A gradual stepwise reduction in food intake by increments of 10% per week was carried out for CR mice. Body weight and food intake were monitored biweekly. CR mice were fed daily between 7.30am ± 1 h and food was placed onto the floor of the cage. AL mice were fed in the hopper. Animal rooms were maintained at 20–22ºC with 30–70% relative humidity and a 12-h light/dark cycle. In March 2013, all animals were moved to the new NIA Biomedical Research Center (across the road), and for the next two weeks, no change in food consumption, bodyweight or unexpected increase in mortality of mice was recorded. For the longevity study, the following mice per group were used: n=50 B6 female and male mice per experimental group, n=63 D2 female AL, n=58 D2 female 20% CR, n=61 D2 female 40% CR, n=60 D2 male AL, n=59 D2 male 20% CR, n=61 D2 male 40% CR. For the F1 study, there were n=72 and n=66 B6D2 male mice on AL and 40% CR diets respectively, while there were n=64 and n=69 D2B6 male mice on AL and 40% CR diets respectively. All animal protocols were approved by the National Institute on Aging Animal Care and Use Committee (405-LEG-2012, 405-TGB-2015, 405-TGB-2019) of the National Institute on Aging.

Survival study

Animals were inspected twice daily for health issues and deaths were recorded for each animal. Moribund animals were euthanized and every animal found dead or euthanized was necropsied. The criteria for euthanasia was based on an independent assessment by a veterinarian according to AAALAC guidelines and only cases, where the condition of the animal was considered incompatible with continued survival, are represented as deaths in the curves. Animals removed at sacrifice were considered as censored deaths. Additional details are provided in the Supplemental Information.

Sacrifice and collection of tissues

At 23–24 months of age (17–18 months of dietary intervention), 6 mice per diet group were sacrificed over three consecutive days from 7am to 11am. Mice were euthanized by cervical dislocation and tissues were rapidly collected, weighed and then snap frozen in liquid nitrogen or processed for further analyses as detailed below. A second cohort of animals (4–6 mice per group, age 17–23 mo, diet 11–17 mo) was anaesthetized with ketamine-xylazine and then oxygenated Krebs–Henseleit buffer was briefly perfused through the liver vasculature at low pressure to wash blood out of the sinusoids. A portion of the liver was fixed for electron microscopy, while the remainder was used for functional autophagy measurements as described below. All mice were sacrificed between 7–11am. On the day of the sacrifice for both cohorts of animals, mice were on their normal feeding cycles, not fasted (mice on a CR diet were not fed their daily ration, while AL mice were allowed to eat *ad libitum* until sacrifice).

Body composition

Measurements of lean, fat and fluid mass in live mice were acquired by nuclear magnetic resonance (NMR) using the Minispec LF90 (Bruker Optics, Billerica, MA).

Rectal temperatures

Rectal temperature was measured in mice with a BAT-12 Microprobe Thermometer with a RET3 rectal probe for mice (Physitemp Instruments, Inc., Clifton, NJ). Additional details are provided in the Supplemental Information.

HOMA calculation

Insulin resistance was calculated from fasted glucose and insulin values using the HOMA2 Calculator software available from the Oxford Centre for Diabetes, Endocrinology and Metabolism, Diabetes Trials Unit website (www.dtu.ox.ac.uk).

Pancreatic islet tissue processing, immunohistochemistry, and image analysis

Paraffin-embedded pancreatic tissue was sectioned, immunostained for insulin and glucagon, and imaged. Quantification of the images was performed using the pancreatic islet analytical software program, Pancreas++. The Supplemental Information contains full methological details.

Gene Expression

Microarray and quantitative RT-PCR techniques were carried out according to standard procedures to determine the effects of sex, gender, and degree of CR on gene expression in mouse liver. Full methodological details are described in Supplemental Experimental Procedures.

Yeast CR experiments and lifespan studies in worms

Chronological aging experiments in wild-type yeast (*S. cerevisiae* BY4741) and respective mutant strains were performed in two types of media defined as SCD and CR media. Lifespan analysis was carried out in two stains of C. elegans supplied with vehicle RNAi or with specific RNAi supplementation as food source. Full methodological details for both invertebrate studies are described in Supplemental Experimental Procedures.

Metabolomics

Metabolomics analysis on mouse liver extracts was performed by the UC Davis Westcoast Metabolomics Center (Davis, CA) according to established procedures (See Supplemental Information for full methological details).

Determination of NAD^+ and hydrogen sulfide levels

The measure of NAD^+ and hydrogen sulfide was carried out in liver extracts according to well-established procedures. Full methodological details are described in the Supplemental Information.

Tissue processing for planimetric and stereological analysis

The left lateral lobe of perfused liver was sectioned and fixed for electron microscopy (EM) to assess general structural preservation and quantification of hepatocyte nuclear size. Whole hepatocyte micrographs were taken for stereological analysis of mitochondrial abundance, and the mitochondrial size and shape was quantified by planimetric analysis. Full methodological details can be found in the Supplemental Information.

Gel Electrophoresis and Western blotting

Separation of mouse liver extracts and mitochondrial preparations for the detection of specific proteins was carried out according to standard procedures as described in the Supplementary Information.

Functional measures of autophagy

Mouse liver lysosomes were isolated from a light mitochondrial–lysosomal fraction in a discontinuous metrizamide density gradient, and a fraction enriched in the subpopulation of lysosomes active for chaperone-mediated autophagy was further separated. Full methodological details for proteolysis by intact lysosomes *in vitro*, LC3 flux, measurement of proteasome activity, and quantification of EM pictures are summarized in Supplemental Information.

Hierarchical clustering

Quantitative behavioral, physiological, biochemical and metabolomics data was z-score normalized across the twelve experimental groups. Unsupervised hierarchical clustering was performed on the normalized data with a custom script using average linkage and uncentered similarity metrics.

Statistics

Data are presented as mean ± SEM unless otherwise specified. Analyses were performed using Excel 2010 (Microsoft), IBM SPSS Statistics (Amonk, NY, USA), or SigmaStat 3.0 (Aspire Software International, San Jose CA). The survival analyses were implemented in R (The R Development Core Team) from scratch using the methodological references given. Comparisons between groups were performed using Student's t-Test or one-way ANOVA with post-hoc tests as specified. Metabolites' analysis from metabolomics data was performed using two-way ANOVA as a function of treatment and sex for each mouse strain with Tukey post hoc analysis. A p value< 0.05 was considered statistically significant. A p value of < 0.05 was considered statistically significant.

Supplementary Material

Refer to Web version on PubMed Central for supplementary material.

Acknowledgments

This work was supported in part by the Intramural Research Program of the National Institute on Aging, NIH, and by NIH grants R01 AG043483 and R01 DK098656 (J.A.B.), NIH grant AG031782 (A.M.C.), the Proteostasis of Aging Core AG038072 (A.M.C.). J.M.M. was supported by a postdoctoral fellowship from the American Diabetes Association, grant 1-15-MI-03. P.C. was supported by NIH grants (1P01AG034906, 1R01GM090311, 1R01ES 020812). F.M. is grateful to the FWF for grants LIPOTOX, I1000, P 27893, P 29203 and P24381-B20 and the BMWFW for grants "Unconventional research" and « Flysleep (80.109/0001 -WF/V/3b/2015). JMV was supported by the Spanish Ministerio de Economía y Competitividad (grants BFU2011-23578 and BFU2015-64630-R). The authors thank the personnel from the Servicio Centralizado de Apoyo a la Investigación (SCAI; University of Córdoba) for technical support. Special thanks to the members of the Translational Gerontology Branch and the Comparative Medicine Section of the National Institute on Aging. In particular we acknowledge Paul Bastian, Elin Lehrmann, Frances Fan, Robin Minor, Dawn Nines and Dawn Boyer.

References

Abu-Bakar A, Lamsa V, Arpiainen S, Moore MR, Lang MA, Hakkola J. Regulation of CYP2A5 gene by the transcription factor nuclear factor (erythroid-derived 2)-like 2. Drug Metab Dispos: the biological fate of chemicals. 2007; 35:787–794.

Adamovich Y, Shlomai A, Tsvetkov P, Umansky KB, Reuven N, Estall JL, Spiegelman BM, Shaul Y. The protein level of PGC-1alpha, a key metabolic regulator, is controlled by NADH-NQO1. Mol Cell Biol. 2013; 33:2603–2613. [PubMed: 23648480]

Anisimov VN, Berstein LM, Egormin PA, Piskunova TS, Popovich IG, Zabezhinski MA, Tyndyk ML, Yurova MV, Kovalenko IG, Poroshina TE, et al. Metformin slows down aging and extends life span of female SHR mice. Cell Cycle. 2008; 7:2769–2773. [PubMed: 18728386]

Anson RM, Guo Z, de Cabo R, Iyun T, Rios M, Hagepanos A, Ingram DK, Lane MA, Mattson MP. Intermittent fasting dissociates beneficial effects of dietary restriction on glucose metabolism and neuronal resistance to injury from calorie intake. Proc Natl Acad Sci U S A. 2003; 100:6216–6220. [PubMed: 12724520]

Artal-Sanz M, Tavernarakis N. Prohibitin couples diapause signalling to mitochondrial metabolism during ageing in C. elegans. Nature. 2009; 461:793–797. [PubMed: 19812672]

Bartke A, Masternak MM, Al-Regaiey KA, Bonkowski MS. Effects of dietary restriction on the expression of insulin-signaling-related genes in long-lived mutant mice. Interdiscip Top Gerontol. 2007; 35:69–82. [PubMed: 17063033]

Barzilai N, Banerjee S, Hawkins M, Chen W, Rossetti L. Caloric restriction reverses hepatic insulin resistance in aging rats by decreasing visceral fat. J Clin Invest. 1998; 101:1353–1361. [PubMed: 9525977]

Berg BN, Simms HS. Nutrition and longevity in the rat. II. Longevity and onset of disease with different levels of food intake. J Nutr. 1960; 71:255–263. [PubMed: 13855553]

Bergamini E, Cavallini G, Donati A, Gori Z. The anti-ageing effects of caloric restriction may involve stimulation of macroautophagy and lysosomal degradation, and can be intensified pharmacologically. Biomed Pharmacother. 2003; 57:203–208. [PubMed: 12888255]

Breese CR, Ingram RL, Sonntag WE. Influence of age and long-term dietary restriction on plasma insulin-like growth factor-1 (IGF-1), IGF-1 gene expression, and IGF-1 binding proteins. J Gerontol. 1991; 46:B180–187. [PubMed: 1716275]

Bruss MD, Khambatta CF, Ruby MA, Aggarwal I, Hellerstein MK. Calorie restriction increases fatty acid synthesis and whole body fat oxidation rates. Am J Physiol Endocrinol Metab. 2010; 298:E108–116. [PubMed: 19887594]

Canto C, Menzies KJ, Auwerx J. NAD(+) Metabolism and the Control of Energy Homeostasis: A Balancing Act between Mitochondria and the Nucleus. Cell Metab. 2015; 22:31–53. [PubMed: 26118927]

Chang HW, Shtessel L, Lee SS. Collaboration between mitochondria and the nucleus is key to long life in Caenorhabditis elegans. Free Radic Biol Med. 2015; 78:168–178. [PubMed: 25450327]

Chattopadhyay M, Kodela R, Nath N, Street CR, Velazquez-Martinez CA, Boring D, Kashfi K. Hydrogen sulfide-releasing aspirin modulates xenobiotic metabolizing enzymes in vitro and in vivo. Biochem Pharmac. 2012; 83:733–740.

Cheney KE, Liu RK, Smith GS, Leung RE, Mickey MR, Walford RL. Survival and disease patterns in C57BL/6J mice subjected to undernutrition. Exp Geront. 1980; 15:237–258.

Ciechanover A. Proteolysis: from the lysosome to ubiquitin and the proteasome. Nat Rev Mol Cell Biol. 2005; 6:79–87. [PubMed: 15688069]

Colman RJ, Anderson RM, Johnson SC, Kastman EK, Kosmatka KJ, Beasley TM, Allison DB, Cruzen C, Simmons HA, Kemnitz JW, et al. Caloric Restriction Delays Disease Onset and Mortality in Rhesus Monkeys. Science. 2009; 325:201–204. [PubMed: 19590001]

Cuervo AM. Autophagy and aging: keeping that old broom working. Trends Gen. 2008; 24:604–612.

Cuervo AM, Dice JF, Knecht E. A population of rat liver lysosomes responsible for the selective uptake and degradation of cytosolic proteins. J Biol Chem. 1997; 272:5606–5615. [PubMed: 9038169]

de Cabo R, Cabello R, Rios M, Lopez-Lluch G, Ingram DK, Lane MA, Navas P. Calorie restriction attenuates age-related alterations in the plasma membrane antioxidant system in rat liver. Exp Geront. 2004; 39:297–304.

DeBalsi KL, Wong KE, Koves TR, Slentz DH, Seiler SE, Wittmann AH, Ilkayeva OR, Stevens RD, Perry CGR, Lark DS, et al. Targeted Metabolomics Connects TXNIP to Mitochondrial Fuel Selection and Regulation of Specific Oxidoreductase Enzymes in Skeletal Muscle. J Biol Chem. 2014; 289(12):8106–8120. [PubMed: 24482226]

Duffy PH, Feuers RJ, Leakey JA, Nakamura K, Turturro A, Hart RW. Effect of chronic caloric restriction on physiological variables related to energy metabolism in the male Fischer 344 rat. Mech Ageing Dev. 1989; 48:117–133. [PubMed: 2661930]

Fernandes G, Yunis EJ, Good RA. Influence of diet on survival of mice. Proc Natl Acad Sci U S A. 1976; 73:1279–1283. [PubMed: 1063408]

Figueroa CD, Taberner PV. Pancreatic islet hypertrophy in spontaneous maturity onset obese-diabetic CBA/Ca mice. Int J Biochem. 1994; 26:1299–1303. [PubMed: 7851633]

Flegal KM, Kit BK, Orpana H, Graubard BI. Association of all-cause mortality with overweight and obesity using standard body mass index categories: a systematic review and meta-analysis. JAMA. 2013; 309:71–82. [PubMed: 23280227]

Flurkey K, Papaconstantinou J, Harrison DE. The Snell dwarf mutation Pit1(dw) can increase life span in mice. Mech Ageing Dev. 2002; 123:121–130. [PubMed: 11718806]

Flurkey K, Papaconstantinou J, Miller RA, Harrison DE. Lifespan extension and delayed immune and collagen aging in mutant mice with defects in growth hormone production. Proc Natl Acad Sci U S A. 2001; 98:6736–6741. [PubMed: 11371619]

Fontana L, Kennedy BK, Longo VD, Seals D, Melov S. Medical research: treat ageing. Nature. 2014; 511:405–407. [PubMed: 25056047]

Fontana L, Partridge L. Promoting health and longevity through diet: from model organisms to humans. Cell. 2015; 161:106–118. [PubMed: 25815989]

Fontana L, Villareal DT, Das SK, Smith SR, Meydani SN, Pittas AG, Klein S, Bhapkar M, Rochon J, Ravussin E, et al. Effects of 2-year calorie restriction on circulating levels of IGF-1, IGF-binding proteins and cortisol in nonobese men and women: a randomized clinical trial. Aging Cell. 2016; 15:22–27. [PubMed: 26443692]

Forster MJ, Morris P, Sohal RS. Genotype and age influence the effect of caloric intake on mortality in mice. FASEB J. 2003; 17:690–692. [PubMed: 12586746]

Gomes AP, Price NL, Ling AJ, Moslehi JJ, Montgomery MK, Rajman L, White JP, Teodoro JS, Wrann CD, Hubbard BP, et al. Declining NAD(+) induces a pseudohypoxic state disrupting nuclear-mitochondrial communication during aging. Cell. 2013; 155:1624–1638. [PubMed: 24360282]

Gomes LC, Di Benedetto G, Scorrano L. During autophagy mitochondria elongate, are spared from degradation and sustain cell viability. Nat Cell Biol. 2011; 13:589–598. [PubMed: 21478857]

Goodrick CL, Ingram DK, Reynolds MA, Freeman JR, Cider N. Effects of intermittent feeding upon body weight and lifespan in inbred mice: interaction of genotype and age. Mech Ageing Dev. 1990; 55:69–87. [PubMed: 2402168]

Grabowski DC, Ellis JE. High body mass index does not predict mortality in older people: analysis of the Longitudinal Study of Aging. J Am Geriatr Soc. 2001; 49:968–979. [PubMed: 11527490]

Gross L, Dreyfuss Y. Reduction in the incidence of radiation-induced tumors in rats after restriction of food intake. Proc Natl Acad Sci U S A. 1984; 81:7596–7598. [PubMed: 6594701]

Guan KL, Xiong Y. Regulation of intermediary metabolism by protein acetylation. Trends Biochem Sci. 2011; 36:108–116. [PubMed: 20934340]

Guevara-Aguirre J, Balasubramanian P, Guevara-Aguirre M, Wei M, Madia F, Cheng CW, Hwang D, Martin-Montalvo A, Saavedra J, Ingles S, et al. Growth hormone receptor deficiency is associated with a major reduction in pro-aging signaling, cancer, and diabetes in humans. Sci Transl Med. 2011; 3:70ra13.

Hansen M, Chandra A, Mitic LL, Onken B, Driscoll M, Kenyon C. A role for autophagy in the extension of lifespan by dietary restriction in C. elegans. PLoS Genet. 2008; 4:e24. [PubMed: 18282106]

Hara T, Nakamura K, Matsui M, Yamamoto A, Nakahara Y, Suzuki-Migishima R, Yokoyama M, Mishima K, Saito I, Okano H, et al. Suppression of basal autophagy in neural cells causes neurodegenerative disease in mice. Nature. 2006; 441:885–889. [PubMed: 16625204]

Harper JM, Leathers CW, Austad SN. Does caloric restriction extend life in wild mice? Aging Cell. 2006; 5:441–449. [PubMed: 17054664]

Harrison DE, Archer JR. Genetic differences in effects of food restriction on aging in mice. J Nutr. 1987; 117:376–382. [PubMed: 3559752]

Harrison DE, Strong R, Allison DB, Ames BN, Astle CM, Atamna H, Fernandez E, Flurkey K, Javors MA, Nadon NL, et al. Acarbose, 17-alpha-estradiol, and nordihydroguaiaretic acid extend mouse lifespan preferentially in males. Aging Cell. 2014; 13:273–282. [PubMed: 24245565]

Harrison DE, Strong R, Sharp ZD, Nelson JF, Astle CM, Flurkey K, Nadon NL, Wilkinson JE, Frenkel K, Carter CS, et al. Rapamycin fed late in life extends lifespan in genetically heterogeneous mice. Nature. 2009; 460:392–395. [PubMed: 19587680]

Hine C, Harputlugil E, Zhang Y, Ruckenstuhl C, Lee BC, Brace L, Longchamp A, Trevino-Villarreal JH, Mejia P, Ozaki CK, et al. Endogenous hydrogen sulfide production is essential for dietary restriction benefits. Cell. 2015; 160:132–144. [PubMed: 25542313]

Hsieh CC, DeFord JH, Flurkey K, Harrison DE, Papaconstantinou J. Effects of the Pit1 mutation on the insulin signaling pathway: implications on the longevity of the long-lived Snell dwarf mouse. Mech Ageing Dev. 2002; 123:1245–1255. [PubMed: 12020946]

Ikeno Y, Hubbard GB, Lee S, Dube SM, Flores LC, Roman MG, Bartke A. Do Ames dwarf and calorie-restricted mice share common effects on age-related pathology? Pathobiol Aging Age Relat Dis. 2013; 3

Kabeya Y, Mizushima N, Ueno T, Yamamoto A, Kirisako T, Noda T, Kominami E, Ohsumi Y, Yoshimori T. LC3, a mammalian homologue of yeast Apg8p, is localized in autophagosome membranes after processing. EMBO J. 2000; 19:5720–5728. [PubMed: 11060023]

Kaushik S, Cuervo AM. Proteostasis and aging. Nat Med. 2015; 21:1406–1415. [PubMed: 26646497]

Khraiwesh H, Lopez-Dominguez JA, Fernandez del Rio L, Gutierrez-Casado E, Lopez-Lluch G, Navas P, de Cabo R, Ramsey JJ, Buron MI, Villalba JM, et al. Mitochondrial ultrastructure and markers of dynamics in hepatocytes from aged, calorie restricted mice fed with different dietary fats. Exp Gerontol. 2014; 56:77–88. [PubMed: 24704714]

Khraiwesh H, Lopez-Dominguez JA, Lopez-Lluch G, Navas P, de Cabo R, Ramsey JJ, Villalba JM, Gonzalez-Reyes JA. Alterations of ultrastructural and fission/fusion markers in hepatocyte mitochondria from mice following calorie restriction with different dietary fats. J Gerontol A Biol Sci Med Sci. 2013; 68:1023–1034. [PubMed: 23403066]

Kirkwood TB. Evolution of ageing. Mech Ageing Dev. 2002; 123:737–745. [PubMed: 11869731]

Kirkwood TB, Shanley DP. Food restriction, evolution and ageing. Mech Ageing Dev. 2005; 126:1011–1016. [PubMed: 15893805]

Kritchevsky D. Caloric restriction and experimental carcinogenesis. Hybrid Hybridomics. 2002; 21:147–151. [PubMed: 12031105]

Kuhla A, Hahn S, Butschkau A, Lange S, Wree A, Vollmar B. Lifelong Caloric Restriction Reprograms Hepatic Fat Metabolism in Mice. J Gerontol A Biol Sci Med Sci. 2013

Lane MA, Ball SS, Ingram DK, Cutler RG, Engel J, Read V, Roth GS. Diet restriction in rhesus monkeys lowers fasting and glucose-stimulated glucoregulatory end points. Am J Physiol. 1995; 268:E941–948. [PubMed: 7762649]

Liao CY, Rikke BA, Johnson TE, Diaz V, Nelson JF. Genetic variation in the murine lifespan response to dietary restriction: from life extension to life shortening. Aging Cell. 2010; 9:92–95. [PubMed: 19878144]

Liao CY, Rikke BA, Johnson TE, Gelfond JAL, Diaz V, Nelson JF. Fat Maintenance Is a Predictor of the Murine Lifespan Response to Dietary Restriction. Aging Cell. 2011a; 10:629–639. [PubMed: 21388497]

Liao CY, Rikke BA, Johnson TE, Gelfond JA, Diaz V, Nelson JF. Fat maintenance is a predictor of the murine lifespan response to dietary restriction. Aging Cell. 2011b; 10:629–639. [PubMed: 21388497]

Longo VD, Antebi A, Bartke A, Barzilai N, Brown-Borg HM, Caruso C, Curiel TJ, de Cabo R, Franceschi C, Gems D, et al. Interventions to Slow Aging in Humans: Are We Ready? Aging Cell. 2015; 14:497–510. [PubMed: 25902704]

Lopez-Lluch G, Hunt N, Jones B, Zhu M, Jamieson H, Hilmer S, Cascajo MV, Allard J, Ingram DK, Navas P, et al. Calorie restriction induces mitochondrial biogenesis and bioenergetic efficiency. Proc Natl Acad Sci U S A. 2006; 103:1768–1773. [PubMed: 16446459]

Madrigal-Matute J, Cuervo AM. Regulation of Liver Metabolism by Autophagy. Gastroenterology. 2016; 150:328–339. [PubMed: 26453774]

Martin-Montalvo A, Mercken EM, Mitchell SJ, Palacios HH, Mote PL, Scheibye-Knudsen M, Gomes AP, Ward TM, Minor RK, Blouin MJ, et al. Metformin improves healthspan and lifespan in mice. Nat Commun. 2013; 4:2192. [PubMed: 23900241]

Masoro EJ. Assessment of nutritional components in prolongation of life and health by diet. Proc Soc Exp Biol Med. 1990; 193:31–34. [PubMed: 2294520]

Masternak MM, Panici JA, Bonkowski MS, Hughes LF, Bartke A. Insulin Sensitivity as a Key Mediator of Growth Hormone Actions on Longevity. J Gerontol A Biol Sci Med Sci. 2009; 64A: 516–521. [PubMed: 19304940]

Mattison JA, Roth GS, Beasley TM, Tilmont EM, Handy AM, Herbert RL, Longo DL, Allison DB, Young JE, Bryant M, et al. Impact of caloric restriction on health and survival in rhesus monkeys from the NIA study. Nature. 2012; 489:318–321. [PubMed: 22932268]

McCay CM, Crowell MF, Maynard LA. The effect of retarded growth upon the length of life span and upon the ultimate body size. 1935. J Nutr. 1935; 10:63–79.

Merkwirth C, Dargazanli S, Tatsuta T, Geimer S, Lower B, Wunderlich FT, von Kleist-Retzow JC, Waisman A, Westermann B, Langer T. Prohibitins control cell proliferation and apoptosis by regulating OPA1-dependent cristae morphogenesis in mitochondria. Genes Dev. 2008; 22:476–488. [PubMed: 18281461]

Miller DL, Roth MB. Hydrogen sulfide increases thermotolerance and lifespan in Caenorhabditis elegans. Proc Natl Acad Sci U S A. 2007; 104:20618–20622. [PubMed: 18077331]

Miller RA, Harrison DE, Astle CM, Baur JA, Boyd AR, de Cabo R, Fernandez E, Flurkey K, Javors MA, Nelson JF, et al. Rapamycin, but not resveratrol or simvastatin, extends life span of genetically heterogeneous mice. J Gerontol A Biol Sci Med Sci. 2011; 66:191–201. [PubMed: 20974732]

Miller RA, Harrison DE, Astle CM, Fernandez E, Flurkey K, Han M, Javors MA, Li X, Nadon NL, Nelson JF, et al. Rapamycin-mediated lifespan increase in mice is dose and sex dependent and metabolically distinct from dietary restriction. Aging Cell. 2014; 13:468–477. [PubMed: 24341993]

Milman S, Atzmon G, Huffman DM, Wan J, Crandall JP, Cohen P, Barzilai N. Low insulin-like growth factor-1 level predicts survival in humans with exceptional longevity. Aging Cell. 2014; 13:769–771. [PubMed: 24618355]

Mitchell SE, Delville C, Konstantopedos P, Derous D, Green CL, Chen L, Han JD, Wang Y, Promislow DE, Douglas A, et al. The effects of graded levels of calorie restriction: III. Impact of short term calorie and protein restriction on mean daily body temperature and torpor use in the C57BL/6 mouse. Oncotarget. 2015a; 6:18314–18337. [PubMed: 26286956]

Mitchell SE, Delville C, Konstantopedos P, Hurst J, Derous D, Green C, Chen L, Han JJ, Wang Y, Promislow DE, et al. The effects of graded levels of calorie restriction: II. Impact of short term calorie and protein restriction on circulating hormone levels, glucose homeostasis and oxidative stress in male C57BL/6 mice. Oncotarget. 2015b; 6:23213–23237. [PubMed: 26061745]

Moreschi C. Beziehungen zwischen Ernahrung und Tumorwachstum. Z fur Immunitatsforsch. 1909; 2:661–675.

Moscovitz O, Ben-Nissan G, Fainer I, Pollack D, Mizrachi L, Sharon M. The Parkinson's-associated protein DJ-1 regulates the 20S proteasome. Nat Commun. 2015; 6:6609. [PubMed: 25833141]

Murtagh-Mark CM, Reiser KM, Harris R Jr, McDonald RB. Source of dietary carbohydrate affects life span of Fischer 344 rats independent of caloric restriction. J Gerontol A Biol Sci Med Sci. 1995; 50:B148–154. [PubMed: 7743394]

Nisoli E, Tonello C, Cardile A, Cozzi V, Bracale R, Tedesco L, Falcone S, Valerio A, Cantoni O, Clementi E, et al. Calorie restriction promotes mitochondrial biogenesis by inducing the expression of eNOS. Science. 2005; 310:314–317. [PubMed: 16224023]

Olzmann JA, Chin LS. Parkin-mediated K63-linked polyubiquitination: a signal for targeting misfolded proteins to the aggresome-autophagy pathway. Autophagy. 2008; 4:85–87. [PubMed: 17957134]

Osborne TB, Mendel LB, Ferry EL. The Effect of Retardation of Growth Upon the Breeding Period and Duration of Life of Rats. Science. 1917; 45:294–295. [PubMed: 17760202]

Pearson KJ, Baur JA, Lewis KN, Peshkin L, Price NL, Labinskyy N, Swindell WR, Kamara D, Minor RK, Perez E, et al. Resveratrol Delays Age-Related Deterioration and Mimics Transcriptional Aspects of Dietary Restriction without Extending Life Span. Cell Metab. 2008a; 8:157–168. [PubMed: 18599363]

Pearson KJ, Lewis KN, Price NL, Chang JW, Perez E, Cascajo MV, Tamashiro KL, Poosala S, Csiszar A, Ungvari Z, et al. Nrf2 mediates cancer protection but not prolongevity induced by caloric restriction. Proc Natl Acad Sci U S A. 2008b; 105:2325–2330. [PubMed: 18287083]

Qiao S, Dennis M, Song X, Vadysirisack DD, Salunke D, Nash Z, Yang Z, Liesa M, Yoshioka J, Matsuzawa S-I, et al. A REDD1/TXNIP pro-oxidant complex regulates ATG4B activity to control stress-induced autophagy and sustain exercise capacity. Nat Commun. 2015; 6

Qiu X, Brown K, Hirschey MD, Verdin E, Chen D. Calorie Restriction Reduces Oxidative Stress by SIRT3-Mediated SOD2 Activation. Cell Metab. 2010; 12:662–667. [PubMed: 21109198]

Rikke BA, Johnson TE. Physiological genetics of dietary restriction: uncoupling the body temperature and body weight responses. Am J Physiol Regul Integr Comp Physiol. 2007; 293:R1522–1527. [PubMed: 17686887]

Rikke BA, Liao CY, McQueen MB, Nelson JF, Johnson TE. Genetic dissection of dietary restriction in mice supports the metabolic efficiency model of life extension. Exp Gerontol. 2010; 45:691–701. [PubMed: 20452416]

Rikke BA, Yerg JE 3rd, Battaglia ME, Nagy TR, Allison DB, Johnson TE. Strain variation in the response of body temperature to dietary restriction. Mech Ageing Dev. 2003; 124:663–678. [PubMed: 12735906]

Rous P. The influence of diet on transplanted and spontaneous tumors. J Exp Med. 1914; 20:433–451. [PubMed: 19867833]

Sadagurski M, Landeryou T, Blandino-Rosano M, Cady G, Elghazi L, Meister D, See L, Bartke A, Bernal-Mizrachi E, Miller RA. Long-lived crowded-litter mice exhibit lasting effects on insulin sensitivity and energy homeostasis. Am J Physiol-Endoc M. 2014; 306:E1305–E1314.

Schneider JL, Suh Y, Cuervo AM. Deficient chaperone-mediated autophagy in liver leads to metabolic dysregulation. Cell Metab. 2014; 20:417–432. [PubMed: 25043815]

Schwer B, Eckersdorff M, Li Y, Silva JC, Fermin D, Kurtev MV, Giallourakis C, Comb MJ, Alt FW, Lombard DB. Calorie restriction alters mitochondrial protein acetylation. Aging Cell. 2009; 8:604–606. [PubMed: 19594485]

Shang Z, Lu C, Chen S, Hua L, Qian R. Effect of H(2)S on the circadian rhythm of mouse hepatocytes. Lipids Health Dis. 2012; 11:23. [PubMed: 22316301]

Sharples AP, Hughes DC, Deane CS, Saini A, Selman C, Stewart CE. Longevity and skeletal muscle mass: the role of IGF signalling, the sirtuins, dietary restriction and protein intake. Aging Cell. 2015; 14:511–523. [PubMed: 25866088]

Sheth SS, Castellani LW, Chari S, Wagg C, Thipphavong CK, Bodnar JS, Tontonoz P, Attie AD, Lopaschuk GD, Lusis AJ. Thioredoxin-interacting protein deficiency disrupts the fasting-feeding metabolic transition. J Lipid Res. 2005; 46:123–134. [PubMed: 15520447]

Shimokawa I, Komatsu T, Hayashi N, Kim SE, Kawata T, Park S, Hayashi H, Yamaza H, Chiba T, Mori R. The life-extending effect of dietary restriction requires Foxo3 in mice. Aging Cell. 2015; 14:707–709. [PubMed: 25808402]

Singh R, Kaushik S, Wang Y, Xiang Y, Novak I, Komatsu M, Tanaka K, Cuervo AM, Czaja MJ. Autophagy regulates lipid metabolism. Nature. 2009; 458:1131–1135. [PubMed: 19339967]

Soare A, Cangemi R, Omodei D, Holloszy JO, Fontana L. Long-term calorie restriction, but not endurance exercise, lowers core body temperature in humans. Aging (Albany NY). 2011; 3:374–379. [PubMed: 21483032]

Solon-Biet SM, Mitchell SJ, Coogan SC, Cogger VC, Gokarn R, McMahon AC, Raubenheimer D, de Cabo R, Simpson SJ, Le Couteur DG. Dietary Protein to Carbohydrate Ratio and Caloric Restriction: Comparing Metabolic Outcomes in Mice. Cell Rep. 2015; 11:1529–1534. [PubMed: 26027933]

Speakman JR, Mitchell SE. Caloric restriction. Mol Aspects Med. 2011; 32:159–221. [PubMed: 21840335]

Strong R, Miller RA, Astle CM, Baur JA, de Cabo R, Fernandez E, Guo W, Javors M, Kirkland JL, Nelson JF, et al. Evaluation of resveratrol, green tea extract, curcumin, oxaloacetic acid, and medium-chain triglyceride oil on life span of genetically heterogeneous mice. J Gerontol A Biol Sci Med Sci. 2013; 68:6–16. [PubMed: 22451473]

Strong R, Miller RA, Astle CM, Floyd RA, Flurkey K, Hensley KL, Javors MA, Leeuwenburgh C, Nelson JF, Ongini E, et al. Nordihydroguaiaretic acid and aspirin increase lifespan of genetically heterogeneous male mice. Aging Cell. 2008; 7:641–650. [PubMed: 18631321]

Sun LY, Spong A, Swindell WR, Fang Y, Hill C, Huber JA, Boehm JD, Westbrook R, Salvatori R, Bartke A. Growth hormone-releasing hormone disruption extends lifespan and regulates response to caloric restriction in mice. eLife. 2013; 2:e01098. [PubMed: 24175087]

Tan JM, Wong ES, Kirkpatrick DS, Pletnikova O, Ko HS, Tay SP, Ho MW, Troncoso J, Gygi SP, Lee MK, et al. Lysine 63-linked ubiquitination promotes the formation and autophagic clearance of protein inclusions associated with neurodegenerative diseases. Hum Mol Genet. 2008; 17:431–439. [PubMed: 17981811]

Tannenbaum A. The initiation and growth of tumors. Introduction. Effects of underfeeding. Am J Cancer. 1940; 38:335–350.

Tauriainen E, Luostarinen M, Martonen E, Finckenberg P, Kovalainen M, Huotari A, Herzig KH, Lecklin A, Mervaala E. Distinct effects of calorie restriction and resveratrol on diet-induced obesity and Fatty liver formation. J Nutr Metab. 2011; 2011:525094. [PubMed: 21977315]

Turturro A, Duffy P, Hass B, Kodell R, Hart R. Survival characteristics and age-adjusted disease incidences in C57BL/6 mice fed a commonly used cereal-based diet modulated by dietary restriction. J Gerontol A Biol Sci Med Sci. 2002; 57:B379–389. [PubMed: 12403793]

Turturro A, Hart RW. Longevity-assurance mechanisms and caloric restriction. Ann N Y Acad Scie. 1991; 621:363–372.

Twig G, Elorza A, Molina AJ, Mohamed H, Wikstrom JD, Walzer G, Stiles L, Haigh SE, Katz S, Las G, et al. Fission and selective fusion govern mitochondrial segregation and elimination by autophagy. EMBO J. 2008; 27:433–446. [PubMed: 18200046]

Weindruch R, Sohal RS. Seminars in medicine of the Beth Israel Deaconess Medical Center. Caloric intake and aging. N Engl J Med. 1997; 337:986–994. [PubMed: 9309105]

Weindruch R, Walford RL, Fligiel S, Guthrie D. The retardation of aging in mice by dietary restriction: longevity, cancer, immunity and lifetime energy intake. J Nutr. 1986; 116:641–654. [PubMed: 3958810]

Weindruch RH, Kristie JA, Cheney KE, Walford RL. Influence of controlled dietary restriction on immunologic function and aging. Fed Proc. 1979; 38:2007–2016. [PubMed: 437143]

Yang G, Zhao K, Ju Y, Mani S, Cao Q, Puukila S, Khaper N, Wu L, Wang R. Hydrogen sulfide protects against cellular senescence via S-sulfhydration of Keap1 and activation of Nrf2. Antiox Redox Signal. 2013; 18:1906–1919.

Yang L, Licastro D, Cava E, Veronese N, Spelta F, Rizza W, Bertozzi B, Villareal DT, Hotamisligil GS, Holloszy JO, et al. Long-Term Calorie Restriction Enhances Cellular Quality-Control Processes in Human Skeletal Muscle. Cell Rep. 2016; 14:422–428. [PubMed: 26774472]

Yuan R, Tsaih SW, Petkova SB, De Evsikova CM, Xing S, Marion MA, Bogue MA, Mills KD, Peters LL, Bult CJ, et al. Aging in inbred strains of mice: study design and interim report on median lifespans and circulating IGF1 levels. Aging Cell. 2009a; 8:277–287. [PubMed: 19627267]

Yuan R, Tsaih SW, Petkova SB, Marin de Evsikova C, Xing S, Marion MA, Bogue MA, Mills KD, Peters LL, Bult CJ, et al. Aging in inbred strains of mice: study design and interim report on median lifespans and circulating IGF1 levels. Aging Cell. 2009b; 8:277–287. [PubMed: 19627267]

Zee RS, Yoo CB, Pimentel DR, Perlman DH, Burgoyne JR, Hou X, McComb ME, Costello CE, Cohen RA, Bachschmid MM. Redox regulation of sirtuin-1 by S-glutathiolation. Antioxid Redox Signal. 2010; 13:1023–1032. [PubMed: 20392170]

Zhang C, Cuervo AM. Restoration of chaperone-mediated autophagy in aging liver improves cellular maintenance and hepatic function. Nat Med. 2008; 14:959–965. [PubMed: 18690243]

Highlights

- Caloric restriction (CR) prevents the age-related decline in proteostasis
- Mitochondrial function is necessary for lifespan extension through CR
- Health and survival outcomes are separated in response to CR in mice
- The CR response depends on strain, sex and level of CR

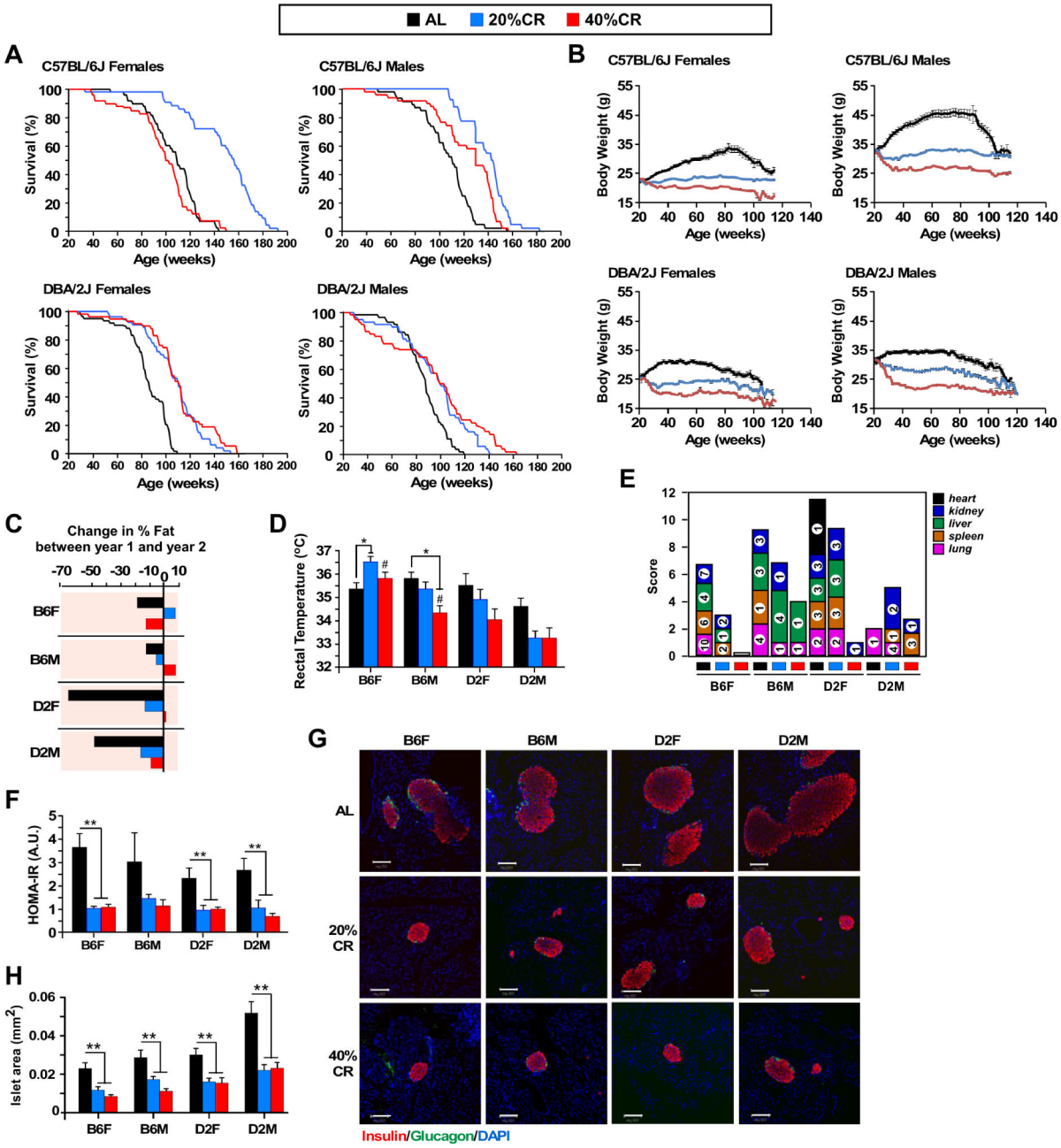

Figure 1. Sex- and strain-specific effects of caloric restriction (CR) on lifespan and healthspan in mice

(A) Kaplan-Meier survival curves for mice fed either a standard diet *at libitum* (AL) or maintained on 20% and 40% CR. n=50–63 mice per experimental group **(B)** Body weight trajectories of mice fed either a standard diet *at libitum* (AL) or maintained on 20% and 40% CR. n=50–63 mice per experimental group **(C)** Change in percent fat mass measured by nuclear magnetic resonance spectroscopy between year-1 and year-2. n=11–50 per experimental group, 11–13 mo age (5–7 mo diet) and 22–24mo age (16–18mo age) **(D)** Rectal temperatures measured in mice. n=8 per experimental group, 18–19 mo age, 12–13

mo on diet **(E)** Prevalence of different grade lymphomas. n=4–12 mice per experimental group. For ages please see Table S3B **(F)** The homeostatic model assessment calculation of insulin resistance (HOMA-IR). n=6 per experimental group, 23–24mo age, 17–18mo on diet **(G)** Immunofluorescence images of pancreatic islets stained for insulin (red; Texas Red) and glucagon (green; FITC). Scale bar, 100 μm. n=6 per experimental group, 23–24mo age, 17–18mo on diet **(H)** Islet area (mm^2) n=4–6 per experimental group, 23–24mo age, 17–18mo on diet. Bars represent mean ± SEM. *, $p<0.05$ compared to AL; $^{\#}$, $p<0.05$ compared to 20% CR.

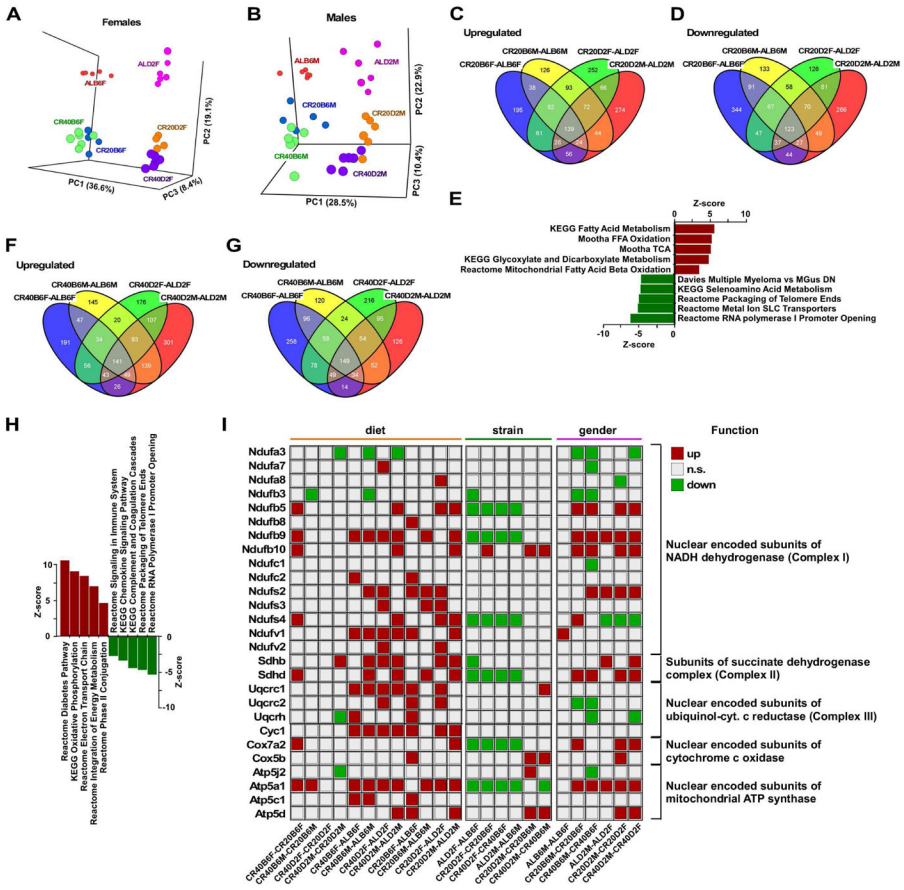

Figure 2. Impact of mouse strain and sex in the global hepatic gene expression profile of mice fed CR versus AL

(A) PCA scatter plot analysis revealed the impact of mouse strain (PC1) and diet (AL versus 20% and 40%CR) (PC2) in female and (**B**) male mice. The difference in pattern between 20%CR and 40%CR was modest, especially in B6 females (PC3). CR40B6F, B6 females on 40%CR; CR20B6F, B6 females on 20%CR; CR40D2F, D2 females on 40%CR; CR20D2F, D2 females on 20%CR; CR40B6M, B6 males on 40% CR; CR20B6M, B6 males on 20% CR; CR40D2M, D2 males on 40%CR; CR20D2M, D2 males on 20%CR. (C) Four-way Venn diagrams of upregulated and (D) downregulated gene transcripts present in CR20B6F-ALB6F, CR20B6M-ALB6M, CR20D2F-ALD2F, and CR20D2M-ALD2M pairwise comparisons. (E) Partial list of top genesets shared among the four CR20-AL pairwise comparisons, with the Z-score values of CR20B6F-ALB6F depicted. (F) Four-way Venn diagrams of upregulated and (G) downregulated gene transcripts present in CR40B6F-ALB6F, CR40B6M-ALB6M, CR40D2F-ALD2F, and CR40D2M-ALD2M pairwise comparisons. (H) Partial list of top genesets shared among the four CR40-AL pairwise comparisons, with the Z-score values of CR40B6F-ALB6F depicted. (I) Binary representation of gene expression related to mitochondrial electron transport chain among all 24 pairwise comparisons. Upregulated (red squares); downregulated (green squares); not significant (beige squares). Listing of the shared gene sets is provided in the Supplemental

Information. All microarray data is n=6 biological replicates per experimental group, 23–24mo age, 17–18mo on diet.

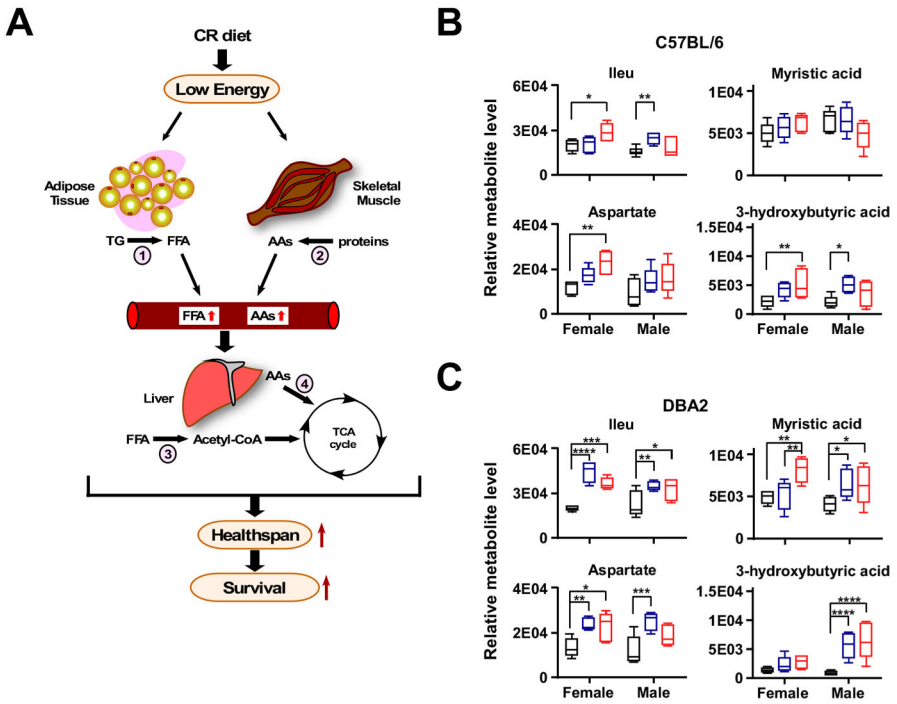

Figure 3. Metabolite profiles in liver of mice on CR indicate the predominance of catabolic modes

(A) Schematic representation of the effect of CR on the release of FFA from adipose tissue (lipolysis, 1) and breakdown of proteins from skeletal muscle (ubiquitin/proteolysis and autophagy, 2), resulting in accumulation of metabolites feeding the TCA cycle in liver mitochondria (fatty acid β-oxidation, 3; anaplerotic filling of the TCA cycle via amino acids, 4). This metabolism switch could account for the increase in healthspan and lifespan observed in CR-fed animals. **(B)** Relative level of Ileu, aspartate, myristate, and 3-hydroxybutyrate in B6 and (**C)** D2 mouse liver is depicted as box plots (n=6 per group). All data is n=6 biological replicates per experimental group, 23–24mo age, 17–18mo on diet. AL, black box, 20% CR, blue box, 40% CR, red box. *, **, *** $P < 0.05$, 0.01 and 0.001.

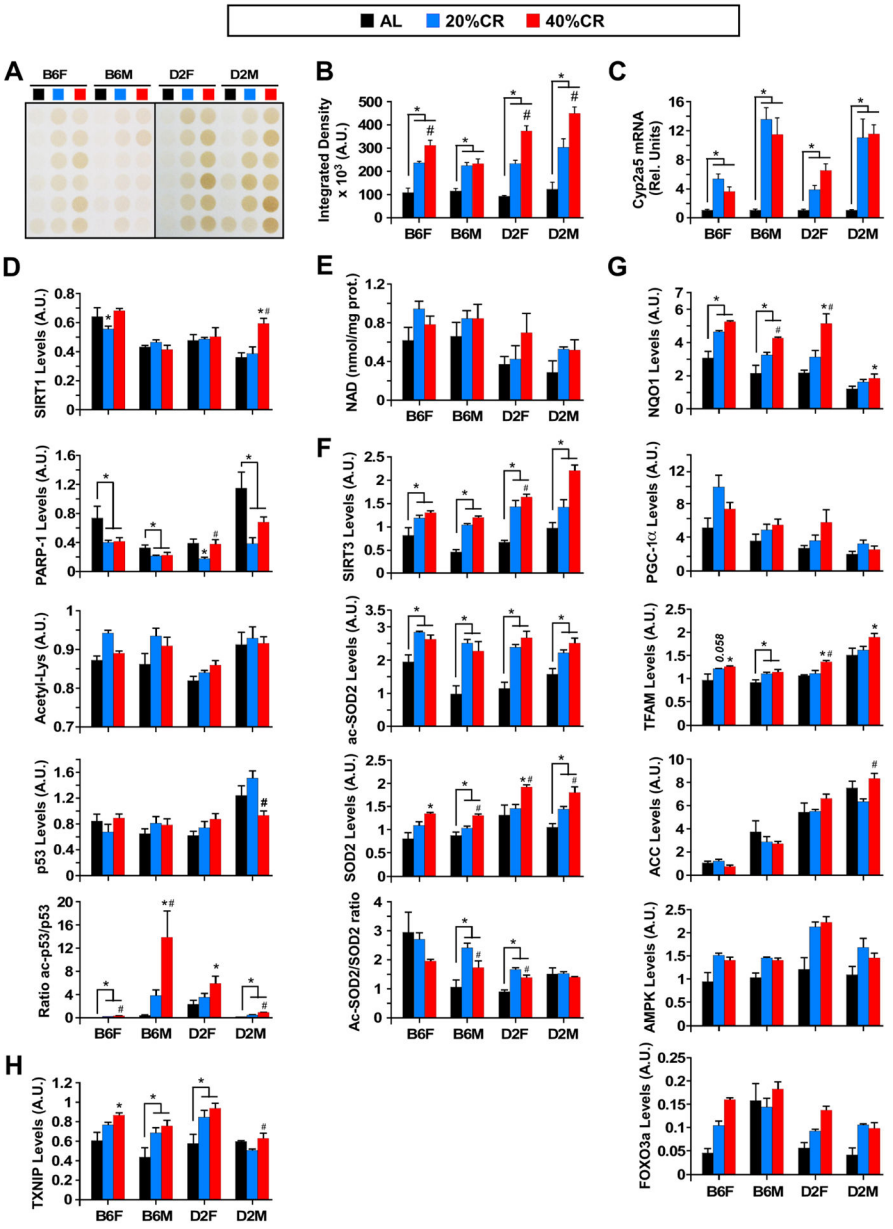

Figure 4. Effect of CR on hydrogen sulfide production and expression of various metabolically relevant protein markers in different mouse strains

(A) Production of H_2S in total liver lysates of AL- and CR-fed mice. **(B)** Densitometric quantification of H_2S production. **(C)** *Cyb2a5* mRNA levels measured by quantitative RT-PCR. **(D)** Total liver lysates were immunoblotted with the indicated primary antibodies (see Figure S3B for full immunoblot images). Densitometric measurements of SIRT1, PARP-1, cellular acetylated proteins, total p53, and ratio of acetylated/total forms of p53 are depicted. (**E**) NAD determination in liver lysates; (**F**) Densitometric measurements of SIRT3, acetylated and total SOD2, and the ratio of acetylated/total forms of SOD2. Full immunoblot images are depicted in Figure S4C. (**G**) Densitometric measurements of NQO1, PGC-1α, TFAM, ACC, AMPK, and FOXO3a are depicted. Full immunoblot images are shown in

Figure S3D. (**H**) Densitometric measurements of TXNIP (full immunoblot images in Figure S3D). (**D-F-H**) Immunoblot membranes were stained with Ponceau S (representative staining in Figure S3E) and each band was normalized to the total densitometric value of the Ponceau staining for that line. All data is the mean ± SEM of 6 biological replicates per experimental group, 23–24mo age, 17–18mo on diet. *, $p<0.05$ compared to AL; #, $p<0.05$ compared to 20% CR.

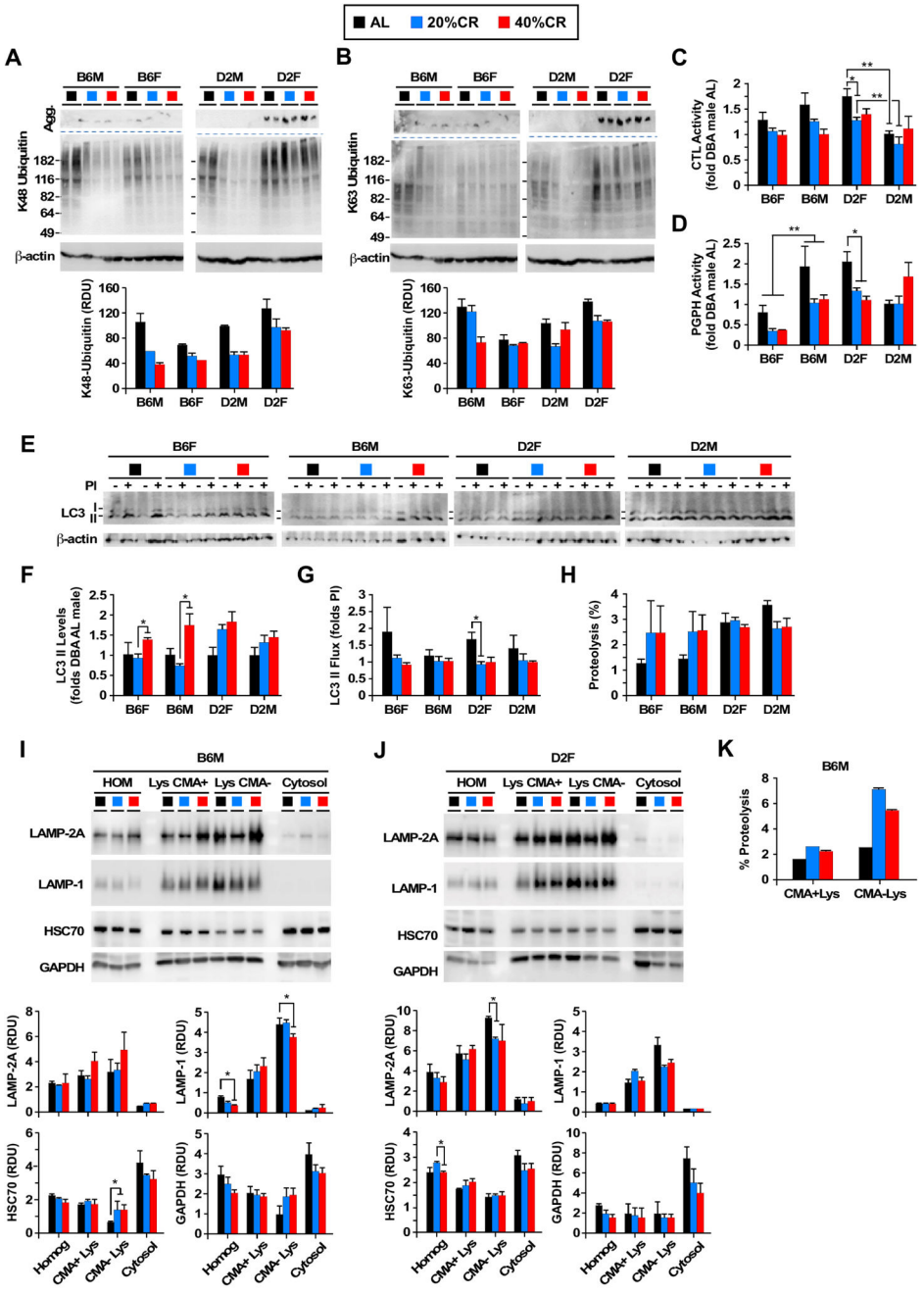

Figure 5. Changes in proteostasis and autophagy in response to CR in different mouse strains

(**A**) Immunoblot for K48- and (**B**) K63-linked ubiquitinated proteins from liver homogenates. *Bottom*: Densitometric quantification after actin normalization. n=2. (**C**) Chymotrypsin-like (CTL) and (**D**) peptidyl-glutamyl peptide-hydrolytic (PGPH) proteasome activity measured in the presence of ATP in liver homogenates. Values are expressed relative to AL-fed D2 males, which were given an arbitrary value of 1. n=3, 23–24mo age, 17–18mo on diet. Values are mean + SEM. *p<0.05, **p<0.01. **(E)** LC3-II levels and LC3-II flux measured by immunoblotting for LC3 in liver explants incubated or not with lysosomal protease inhibitors (PI, NH_4Cl and leupeptin). **(F)** Graphs show densitometric quantification

of LC3 levels and **(G)** LC3 II flux. n=4, 23–24mo age, 17–18mo on diet. **(H)** CMA activity as measured by percentage of proteolysis of radiolabeled pool of cytosolic proteins in isolated intact CMA+ lysosomes. n=2, 23–24mo age, 17–18mo on diet. **(I)** Immunoblot for the indicated proteins in homogenate (HOM), CMA+ and CMA- lysosomes, and cytosol isolated from livers of B6 males and (**J**) D2 females. Graphs (*bottom*) show densitometric quantification of LAMP-2A, LAMP-1, HSC70 and GAPDH. **(K)** CMA activity as measured as in **I** in CMA+ (n=2) and CMA-lysosomes isolated from B6 male mice (n=3–4). Values are mean ± SEM, 23–24mo age, 17–18mo on diet. *p<0.05, **p<0.01, ***p<0.001.

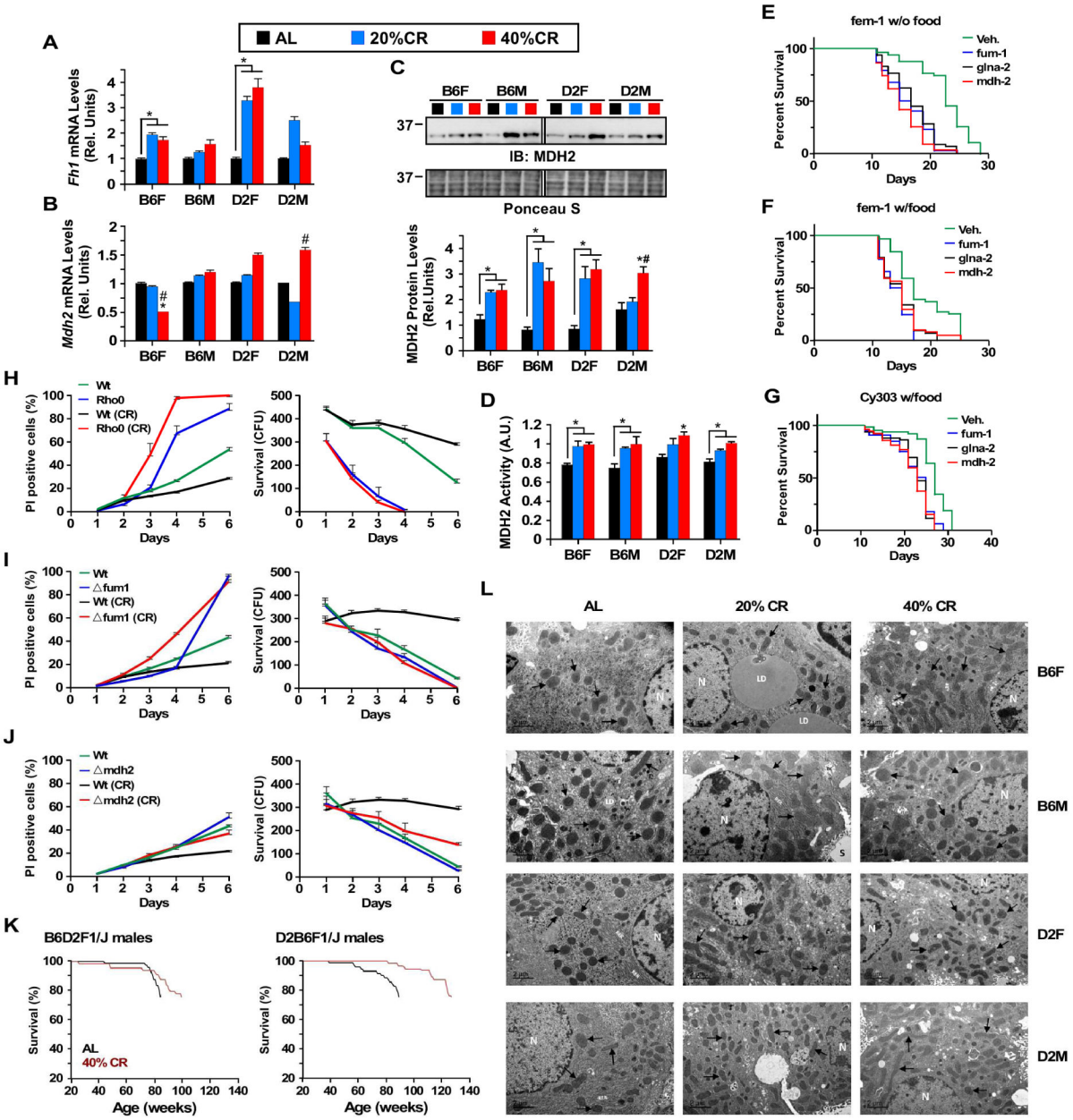

Figure 6. Functional mitochondria are required for the lifespan extension effects of CR

(A) *Fh1* and (**B**) *Mdh2* mRNA levels were measured by quantitative RT-PCR. Bars represent mean ± SEM of 4–6 biological replicates, 23–24mo age, 17–18mo on diet. *, $p<0.05$ compared to AL; #, $p<0.05$ compared to 20% CR. **(C)** Mdh2 protein levels and (**D**) activity in total liver lysates. **(E–F)** Survival curves of fem-1 and (**G**) Cy303 strains of C. elegans harboring genetic deletion either in *fum-1*, *glna-2* or *mdh2*. **(H)** Survival curves (right panels) and percent of PI-stained cells (left panels) of rho0, (**I**) Δfum1, and (**J**) Δmdh2 yeast cell mutants fed either AL or CR diet. (**K**) Kaplan-Meier survival curves for B6D2F1/J and D2B6F1/J male mice fed either a standard diet *at libitum* (AL) or maintained on 40% CR. n=60–75 mice per experimental group **(L)** Representative transmission electron microscopy

images of liver sections of all 12 experimental groups, n=4–6 biological replicates per experimental group, 23–24mo age, 17–18mo on diet.

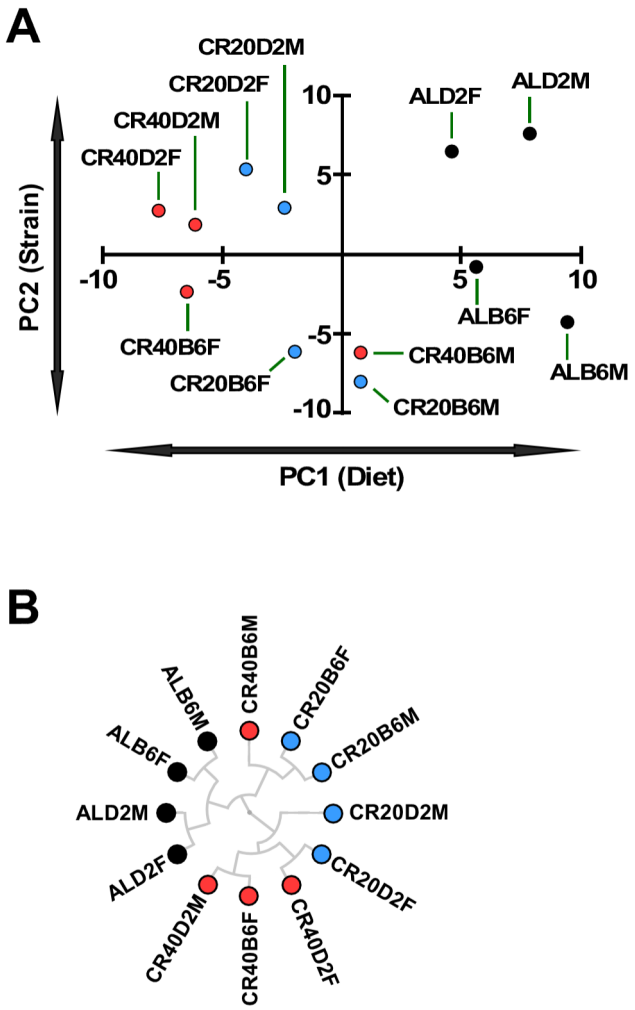

Figure 7.

Principal component analysis (**A**) and hierarchical clustering (**B**) of the various experimental groups based on Z-score normalized behavioral, physiological, biochemical and metabolomics data using uncentered similarity metrics and average linkage (see Figure S7 for a clustering of the input data).